POLITECNICO DI MILANO

Facoltà di Ingegneria Industriale
Corso di Laurea in Ingegneria Aeronautica

Riemann problem for dissociating hydrogen gas

Relatore: Prof. Luigi Quartapelle

Enrico Rinaldi 729906

Anno Accademico 2009/2010

Contents

List of Figures

List of Tables

Sommario

L'obiettivo di questa tesi è lo studio del problema di Riemann della gasdinamica in un gas diatomico che dissocia. L'attenzione sarà concentrata sul gas di idrogeno. Nonostante l'idrogeno non sia coinvolto nelle tipiche correnti ipersoniche nelle fasi di rientro atmosferico, la scelta è comunque giustificata dalle sue numerose applicazioni tecnologiche. Inoltre, diversi studi di carattere astrofisico coinvolgono il gas idrogeno che attraversa un ampio intervallo di temperature fino alla ionizzazione.

Da un punto di vista termodinamico l'idrogeno è molto interessante a causa del valore piuttosto elevato della sua *temperatura rotazionale* che consente agli effetti dovuti alle rotazioni molecolari di manifestarsi a temperature non troppo basse.

In questo lavoro è stato utilizzato un modello termodinamico recentemente introdotto da Quartapelle e Muzzio [1] (si veda anche [2]) che tiene correttamente in conto l'accoppiamento tra rotazioni e vibrazioni anarmoniche della molecola H_2, descritte tramite il potenziale di Morse [3]. Inoltre, la dissociazione molecolare viene rappresentata come un aspetto puramente termodinamico che avviene in seguito a rotazioni o vibrazioni non più sostenibili, abbandonando quindi la *legge di azione di massa* spesso impiegata per determinare la composizione all'equilibrio di una miscela. L'attenzione di questa tesi è rivolta all'introdurre questo concetto nella risoluzione del problema di Riemann. I risultati ottenuti verranno confrontati con quelli forniti da un modello termodinamico semplificato che considera le rotazioni completamente eccitate. L'analisi non sarà limitata solamente ai valori di temperatura elevati ai quali avviene la dissociazione, ma si rivolgerà anche al dominio delle basse temperature alle quali la distinzione tra i due modelli termodinamici diventa marcata. Sebbene già in condizioni di dissociazione le differenze tra i risultati forniti dai due modelli inducano all'utilizzo di quello completo, quando lo sguardo si sposta sulle basse temperature la scelta diventa obbligata.

Il capitolo 2 descrive il modello termodinamico completo per l'idrogeno, che include l'accoppiamento tra rotazioni e vibrazioni della molecola e la sua dissociazione (RVD). Sono inoltre derivate le espressioni di tutte le proprietà termodinamiche necessarie nella soluzione del problema di Riemann, come funzioni di temperatura T e volume specifico v.

Il capitolo 3 richiama i principi fondamentali di due modelli semplificati, entrambi caratterizzati da un trattamento *classico* delle rotazioni. Il primo modello condivide con quello completo le vibrazioni anarmoniche e la dissociazione (VD) mentre il secondo è basato su oscillazioni armoniche e utilizza la legge di azione di massa per determinare la composizione del gas. Sono inoltre effettuati dei confronti sulle proprietà termodinamiche più importanti ottenuti con i vari modelli.

Il capitolo 4 è la parte più originale del lavoro ed è dedicata allo studio del problema di Riemann per un gas diatomico che dissocia. In primo luogo sono evidenziati i tratti essenziali del problema di Riemann, come prensentato in [4]. In seguito si fornisce una nuova e completa formulazione del problema, estesa al gas in presenza di dissociazione. Quest'ultima rende il problema matematico più complicato e richiede la soluzione di sistemi non lineari all'interno del ciclo principale che determina gli stati sinistro e destro sulla discontinuità di contatto. In particolare, sia la soluzione dell'onda d'urto che dell'onda di rarefazione richiedono di risolvere un sistema formato da due equazioni che sono l'equazione che definisce il coefficiente di dissociazione e, rispettivamente, l'equazione di Rankine–Hugoniot o la condizione di entropia costante.

Nel capitolo 5 sono presentati e commentati i risultati più significativi dei problemi di Riemann analizzati. Particolare attenzione è dedicata alle situazioni in cui la dissociazione gioca un ruolo importante, quindi alle alte temperature. Per verificare l'accuratezza dei risultati è effettuato un confronto tra quelli ottenuti con il modello RVD e VD. Inoltre, nel caso delle onde d'urto, è possibile confrontare le soluzioni con i dati forniti dalla NASA [5]. Infine viene analizzata la regione di basse temperature sia per le onde d'urto che di rarefazione, in modo da evidenziare le differenze che scaturiscono da un differente trattamento delle rotazioni.

Il capitolo 6 riassume il lavoro fatto e le conclusioni che si possono trarre, proponendo infine possibili sviluppi futuri.

Infine l'appendice A presenta le espressioni delle funzioni di partizione utilizzate nei modelli RVD e VD.

1 Introduction

The Riemann problem of gasdynamics is very important in the study of nonlinear waves in compressible flows and it is also fundamental in the development of finite volume methods in which it occurs at every interface between two grid cells. Generally, the Riemann problem for gases with simple thermodynamic properties is studied. On the other hand, taking into account molecular dissociation is mandatory for hypersonic flows in which the rise in temperature after the shock front leads to a modification in the chemical composition of the gas.

The aim of this work is to study the Riemann problem in a diatomic gas in the presence of dissociation. The focus will be on the hydrogen gas. Even if the hydrogen is not involved in typical hypersonic flows in the re-entry phase, the choice is justified by its many technological applications (a typical Riemann problem of general interest involving hydrogen gas could be the failure of a pipe). Besides that, many astrophysical investigations involve the hydrogen gas encompassing a wide range of temperatures up to ionization.

From a thermodynamical viewpoint, the hydrogen gas is very interesting because of the fairly large value of its *rotational temperature*, so that the peculiar effects of molecular rotations can manifest at not too small temperatures. An original and recent thermodynamic model due to Quartapelle and Muzzio [1] (see also [2]) which properly takes into account effects of rotations and the dissociation of the molecule H_2 will be used. The focus of the present work will be the inclusion of the dissociation as a purely thermodynamic aspect in the Riemann problem, abandoning the *law of mass action* commonly employed to determine the composition of the gas. Furthermore, the Riemann problem in the low temperature region will be analyzed in order to understand the improvements stemming from the complete model with a coupled treatment of rotations and anharmonic vibrations, with respect to a simplified model which considers fully excited rotations.

Chapter 2 describes the complete thermodynamic model for the hydrogen gas including the rotations and vibrations of the molecules and their dissociation (RVD) into atoms, as presented in [1, 2]. The expressions of all the thermodynamic properties of the gas needed for formulating the Riemann problem are derived as functions of the temperature T and the specific volume v.

Chapter 3 recalls the basic elements of two simplified models, both characterized by fully excited molecular rotations. The first model shares with the complete one the anharmonic vibrations and dissociation (VD) while the second approximate model is based on harmonic oscillations (HC) but must be complemented by the chemical law of mass action to account for molecular dissociation.

Chapter 4 is most the original contribution of the work and is devoted to the

study of the Riemann problem for a dissociating diatomic ideal gas. First, the fundamental features of the Riemann problem of the gasdynamics are oulined, as presented in [4]. Then a new and complete formulation of this problem in the context of a dissociating ideal gas is presented. The presence of the dissociation coefficient makes actually the mathematical problem more difficult than for a nondissociating gas and may require to solve nonlinear systems within the external cycle which determines the states on the two sides of the contact discontinuity. In particular, the solution of either the rarefaction wave or the shock wave is obtained from nonlinear systems of two equations representing the dissociation equation and the condition of constant entropy or the Rankine–Hugoniot equation, respectively.

In chapter 5 the most important results of the Riemann problems are presented and discussed. Particular attention is payed to situations in which the dissociation plays an important role, thus high temperature values are considered. In order to verify the accuracy of the solutions, a comparison between the results obtained by means of RVD and VD models is made. For the case of the shock waves, a comparison with data provided by NASA [5] is also possible. Finally, the domain of low temperatures is analyzed for either shock or rarefaction waves to underline the differences resulting from different treatment of rotations.

Chapter 6 summarizes all the work done and the results obtained, and proposes some future developments.

Finally, appendix A presents the expressions of the partition functions used for the RVD and VD models.

2 Thermodynamics of hydrogen gas at equilibrium

This chapter recalls the basic elements of the thermodynamic model due to Quartapelle and Muzzio described in [1] and detailed in the appendix RV of the lecture notes [2]. The model describes a dissociating diatomic ideal gas under the assumption of thermodynamic equilibrium. The internal motion of the diatomic molecules is characterized by a complete coupling between rotations and anharmonic vibrations, as described in appendix A.

First the Helmholtz potential is introduced and the condition for equilibrium dissociation is considered to define the dissociation coefficient α of the diatomic gas, which is uniquely determined by the temperature T and the specific volume v. Next, the Helmholtz potential is used to derive the equations of state for energy, entropy and other relevant thermodynamic properties, as functions of T and v.

2.1 Helmholtz potential

As is well known, the Helmholtz potential (also referred to as Helmholtz free energy) is a thermodynamic potential obtained by performing a Legendre transform on the fundamental relation in the energetic representation[1] in order to have T and V as independent variables. The expression of the free energy for the gas considered is:

$$F(T, V, \tilde{N}_{\mathrm{H_2}}, \tilde{N}_{\mathrm{H}}) = -\tilde{N}_{\mathrm{H_2}}\, k_{\mathrm{B}} T \ln \frac{\mathrm{e} Z_{\mathrm{H_2}}(T, V)}{\tilde{N}_{\mathrm{H_2}}} - \tilde{N}_{\mathrm{H}}\, k_{\mathrm{B}} T \ln \frac{\mathrm{e} Z_{\mathrm{H}}(T, V)}{\tilde{N}_{\mathrm{H}}}, \quad (2.1)$$

with the partition functions $Z_{\mathrm{H_2}}(T, V)$ and $Z_{\mathrm{H}}(T, V)$ expressed by equations (A.15) and (A.16), respectively. Here "e" denotes the base of the natural logarithm and $\tilde{N}_{\mathrm{H_2}}$ and $\tilde{N}_{\mathrm{H}}$ the number of the molecules H_2 and atoms H. The free energy (2.1) is a fundamental thermodynamic relation and all the thermodynamic properties of the gas can be obtained from it. Moreover, the minimum of F defines the equilibrium composition of the gas which undergoes a chemical transformation.

2.2 Equilibrium dissociation

Following Zel'dovich and Raizer [8], the equilibrium composition of the gas stems from two constraints which express the stationarity of F and the conservation of

[1] $E = E(S, V, \tilde{\mathbf{N}})$ with E, S, V and $\tilde{\mathbf{N}} = (\tilde{N}_1, \tilde{N}_2, \dots)$ denoting respectively the internal energy, the entropy, the volume and the total number of particles. For a complete description of the fundamental relation in both energetic and entropic form and its mathematical properties we refer to [6, 7].

the atomic constituents of the gas mixture through the relation $2\tilde{N}_{\mathrm{H}_2} + \tilde{N}_{\mathrm{H}} = \tilde{\mathcal{N}}_{\mathrm{H}}$, where $\tilde{\mathcal{N}}_{\mathrm{H}}$ denotes the (fixed) total number of constituents present either as free atoms H or as atomic components of the molecules H_2. Using this two conditions leads to:

$$\frac{\tilde{N}_{\mathrm{H}}^2}{\tilde{N}_{\mathrm{H}_2}} = \frac{Z_{\mathrm{H}}^2}{Z_{\mathrm{H}_2}}. \tag{2.2}$$

Let us now introduce the dissociation coefficient α:

$$\alpha \equiv \frac{\tilde{\mathcal{N}}_{\mathrm{H}_2} - \tilde{N}_{\mathrm{H}_2}}{\tilde{\mathcal{N}}_{\mathrm{H}_2}}, \tag{2.3}$$

from which we can find:

$$\tilde{N}_{\mathrm{H}_2} = (1-\alpha)\tilde{\mathcal{N}}_{\mathrm{H}_2} \qquad \text{and} \qquad \tilde{N}_{\mathrm{H}} = 2\alpha\tilde{\mathcal{N}}_{\mathrm{H}_2}. \tag{2.4}$$

Substituting the partition functions (A.15) and (A.16) into the equilibrium equation (2.2) and using the relationships (2.4), gives:

$$\frac{\alpha^2}{1-\alpha} = \frac{1}{4}\frac{Z_{\mathrm{H}}^2(T,V)}{Z_{\mathrm{H}_2}(T,V)}\frac{1}{\tilde{\mathcal{N}}_{\mathrm{H}_2}} = \frac{t^{3/2}\,\mathrm{e}^{-t_{\mathrm{d}}/t}}{z_{\mathrm{rv}}^{\mathrm{nuc}}(t)}\frac{v}{v_{\mathrm{d}}^*} \equiv \beta(t,v), \tag{2.5}$$

with $v = V\,/\,[m_{\mathrm{H}_2}\tilde{\mathcal{N}}_{\mathrm{H}_2}]$, $t = T/T_{\mathrm{v}}$, $z_{\mathrm{rv}}^{\mathrm{nuc}}(t) = \mathrm{e}^{-D_e/k_{\mathrm{B}}T} Z_{\mathrm{rv}}^{\mathrm{nuc}}(T)$ and $Z_{\mathrm{rv}}^{\mathrm{nuc}}(T)$ given by equation (A.12), and where we have introduced the constants:

$$\frac{1}{v_{\mathrm{d}}^*} = \frac{(2I_{\mathrm{H}}+1)^2}{4\sqrt{2}}\frac{(g_{\mathrm{H}}^0)^2 H^{5/2}}{g_{\mathrm{H}_2}^0}\,T_{\mathrm{v}}^{3/2}\frac{(2\pi k_{\mathrm{B}})^{3/2}\,u^{5/2}}{h^3},$$
$$t_{\mathrm{d}} = \frac{n_{\max}}{2+1/n_{\max}},$$

with H the hydrogen mass in atomic unit, $u = 1.660 \times 10^{-27}$ kg, and the other quantities defined in appendix A. Solving equation (2.5) for α gives the equilibrium dissociation coefficient of the gas:

$$\alpha(t,v) = \frac{1}{2}\beta(t,v)\left[\sqrt{1+4/\beta(t,v)} - 1\right]. \tag{2.6}$$

2.3 Energy equation of state

The internal energy of the mixture is defined by the standard relation:

$$E = F(T,V,\tilde{N}_{\mathrm{H}_2},\tilde{N}_{\mathrm{H}}) - T\frac{\partial F(T,V,\tilde{N}_{\mathrm{H}_2},\tilde{N}_{\mathrm{H}})}{\partial T}, \tag{2.7}$$

with F given by equation (2.1). A direct calculation provides the dimensionless specific internal energy $\epsilon \equiv e/[R_{\mathrm{H}_2} T_{\mathrm{v}}]$ of the dissociating gas as a function of t and α:

$$\epsilon^{\mathrm{f}}(t,\alpha) = \frac{3}{2}\,(1+\alpha)\,t + (1-\alpha)\,[\epsilon_{\mathrm{rv}}(t) - t_{\mathrm{d}}],$$

where the superscript $^{\mathrm{f}}$ underlines that ϵ^{f} is the energy of the *frozen* mixture, namely a function also of α as an independent variable. Moreover, $\epsilon_{\mathrm{rv}}(t) = x_{\mathrm{rv}}(t)/z_{\mathrm{rv}}(t)$ is the roto-vibrational contribution to the internal energy, with $x_{\mathrm{rv}}(t) \equiv z'_{\mathrm{rv}}(t)\,t^2$. At thermodynamic equilibrium, the dissociation coefficient is given by (2.6), so that the specific energy depends on both the independent variables t and v:

$$\epsilon(t,v) = \frac{3}{2}\,[1+\alpha(t,v)]\,t + [1-\alpha(t,v)]\,[\epsilon_{\mathrm{rv}}(t) - t_{\mathrm{d}}]. \tag{2.8}$$

2.4 Entropy equation of state

The entropy is defined from the Helmholtz free energy F by:

$$S = -\frac{\partial F(T, V, \tilde{N}_{\mathrm{H}_2}, \tilde{N}_{\mathrm{H}})}{\partial T}. \tag{2.9}$$

A direct calculation provides the dimensionless specific entropy $\sigma \equiv s/R_{\mathrm{H}_2}$ of the dissociating gas as a function of t, v and α:

$$\sigma^{\mathrm{f}}(t,v,\alpha) = (1+\alpha)\left[\frac{5}{2} + \frac{3}{2}\,\ln t + \ln\left(\frac{v}{v^*_{\mathrm{d}}}\right)\right] + (1-\alpha)\,\sigma_{\mathrm{rv}}(t) + \Upsilon(\alpha) + \sigma_0,$$

where σ_0 is the entropy in a reference state, $\sigma_{\mathrm{rv}}(t) = \frac{x_{\mathrm{rv}}(t)}{t\,z_{\mathrm{rv}}(t)} + \ln z_{\mathrm{rv}}(t)$ is the roto-vibrational contribution to the entropy and $\Upsilon(\alpha) \equiv -2\alpha\ln\alpha - (1-\alpha)\ln(1-\alpha)$ is the contribution due to the mixing of the molecular and atomic species.

Taking into account the equilibrium dissociation leads to the entropy equation of state:

$$\begin{aligned}\sigma(t,v) = {} & [1+\alpha(t,v)]\left[\frac{5}{2} + \frac{3}{2}\,\ln t + \ln\left(\frac{v}{v^*_{\mathrm{d}}}\right)\right] \\ & + [1-\alpha(t,v)]\,\sigma_{\mathrm{rv}}(t) + \Upsilon(\alpha(t,v)) + \sigma_0.\end{aligned} \tag{2.10}$$

2.5 Thermodynamic properties

From the explicit expression of the Helmholtz potential and of the equations of state for energy and entropy, any other thermodynamic property of the gas can be derived. Since we are interested in the equilibrium properties, hereinafter we will always consider $\alpha = \alpha(t,v)$ avoiding to write the independent variables t and v.

2.5.1 Pressure

The pressure function can be obtained from the Helmholtz potential by means of

$$P = -k_{\mathrm{B}} T \frac{\partial F(T, V, \tilde{N}_{\mathrm{H_2}}, \tilde{N}_{\mathrm{H}})}{\partial V}. \tag{2.11}$$

A direct calculation leads to:

$$P(T, v) = (1 + \alpha)\, \frac{R_{\mathrm{H_2}} T}{v}. \tag{2.12}$$

It is useful to express the derivatives of the scaled pressure $p = P/[R_{\mathrm{H_2}} T_{\mathrm{v}}]$ with respect to t and v:

$$\begin{aligned} \frac{\partial p(t, v)}{\partial t} &= (1 + \alpha + t\alpha_t)\, \frac{1}{v}, \\ \frac{\partial p(t, v)}{\partial v} &= -\,(1 + \alpha - v\alpha_v)\, \frac{t}{v^2}, \end{aligned}$$

where α_t and α_v denote the partial derivatives of $\alpha(t, v)$. The pressure derivatives are now used to derive other thermodynamic properties that will be employed in the solution of the Riemann problem to be discussed in chapter 4.

2.5.2 Specific heats

First, we consider the specific heat at constant volume, which is defined as the partial derivative of the specific internal energy with respect to the temperature:

$$c_v(T, v) = \frac{\partial e(T, v)}{\partial T} = \frac{\partial e^{\mathrm{f}}(T, \alpha)}{\partial T} + \frac{\partial e^{\mathrm{f}}(T, \alpha)}{\partial \alpha} \alpha_T(T, v). \tag{2.13}$$

Substituting the expressions of the derivatives of the internal energy yields:

$$\frac{c_v(t, v)}{R_{\mathrm{H_2}}} = \frac{3}{2}\,(1 + \alpha) + (1 - \alpha)\, \epsilon'_{\mathrm{rv}}(t) + \left[\frac{3}{2} t - [\epsilon_{\mathrm{rv}}(t) - t_{\mathrm{d}}]\right] \alpha_t \tag{2.14}$$

where $\epsilon'_{\mathrm{rv}}(t) = [z_{\mathrm{rv}}(t)\, y_{\mathrm{rv}}(t) - x_{\mathrm{rv}}(t)] \,/\, [t\, z_{\mathrm{rv}}(t)]^2$ with $y_{\mathrm{rv}}(t) = t^2\, x'_{\mathrm{rv}}(t)$. The specific heat at constant pressure is defined as follows

$$c_P = c_v - T \left(\frac{\partial v}{\partial T}\right)_P^2 \Bigg/ \left(\frac{\partial v}{\partial P}\right)_T,$$

where the derivative $(\partial v/\partial T)_P$ is obtained from the pressure equation of state $P = P(T, v)$ by implicit differentiation. For the case of the dissociating diatomic ideal gas considered, it yields:

$$c_P(t, v) = c_v(t, v) + \frac{(1 + \alpha + t\alpha_t)^2}{1 + \alpha - v\alpha_v}. \tag{2.15}$$

Figures 1 and 2 show the temperature dependence of $c_v(T, v)$ and $c_P(T, v)$, for different values of the specific volume. For temperatures up to $600\ \mathrm{K}$, equilibrium hydrogen c_P agrees well with values provided by [9], with relative differences $< 1\%$. In the low temperature range, c_v and c_P have the well known behaviour for the diatomic hydrogen gas at equilibrium, as presented for example in [10], with a difference in the position of the maximum value $< 1\%$.

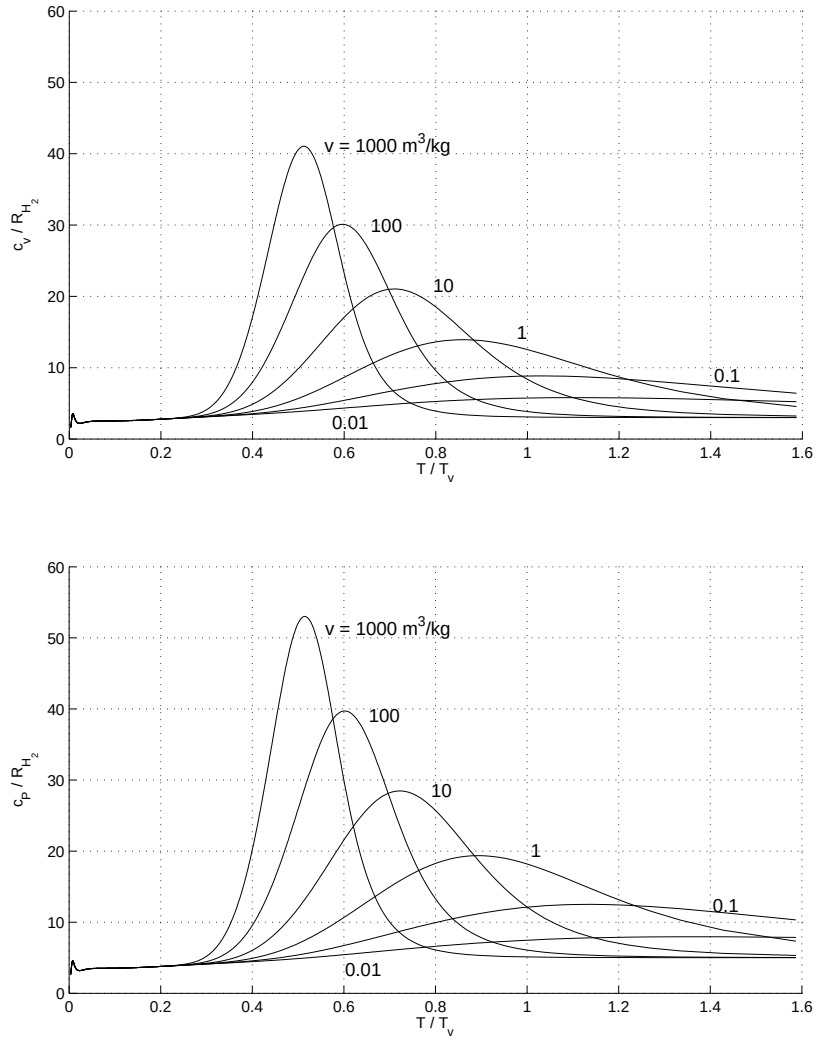

Figure 1: Specific heats $c_v(T, v)$ (upper) and $c_P(T, v)$ (lower) for different values of the specific volume v.

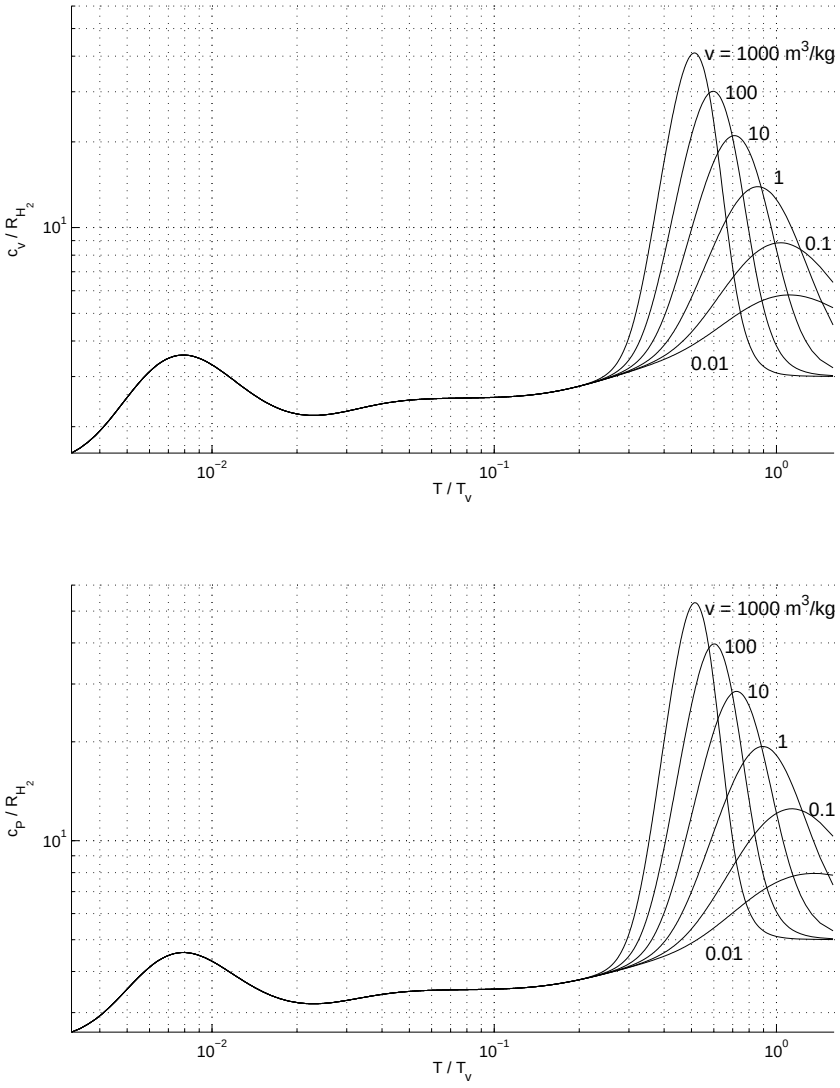

Figure 2: Specific heats $c_v(T, v)$ (upper) and $c_P(T, v)$ (lower) in logarithmic scale, for different values of the specific volume.

In the low temperature region it is important to distinguish between ortho- and parahydrogen. The orthohydrogen molecules have two nuclei with parallel spin, whereas parahydrogen molecules have nuclei with antiparallel spin. For very low temperatures (about $20\,\mathrm{K}$), the hydrogen gas is composed almost completely by parahydrogen and at about $80\,\mathrm{K}$ the composition is near to 50%. As temperature increases, the ratio between orthohydrogen and parahydrogen tends to $3:1$: this distribution ratio is commonly defined as normal hydrogen. To represent the ortho- and para- modifications, the summation over the rotational quantum numbers in the roto-vibration partition function (A.15) must be limited to j odd for orthohydrogen and j even for parahydrogen. In figure 3 both specific heats are plotted for ortho-, para- and normal hydrogen. Curves are in excellent accord with the known behaviour, presented for example in [11]. The values of c_P for parahydrogen and orthohydrogen are compared with data presented in [9], showing relative differences $< 1\%$.

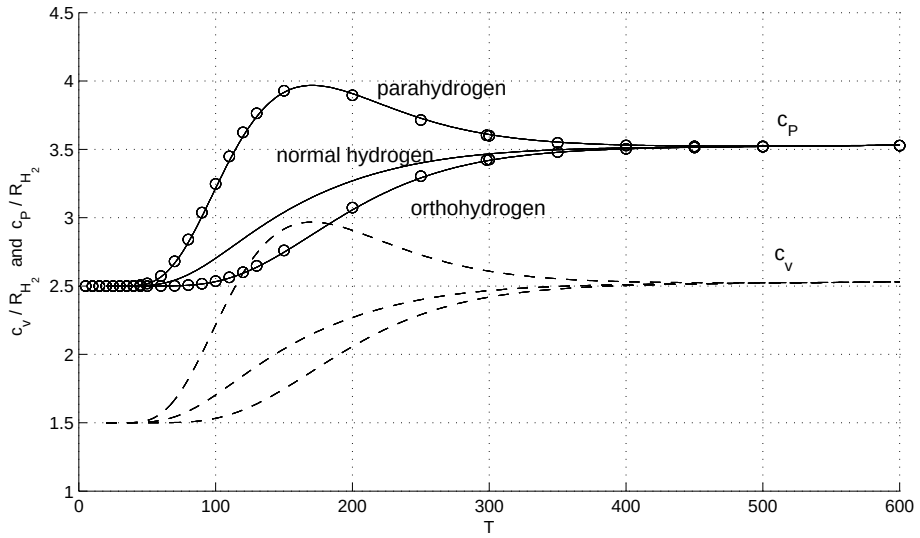

Figure 3: Specific heats $c_v(T, v)$ (solid) and $c_P(T, v)$ (dashed) for the orthohydrogen, parahydrogen and normal hydrogen. Circles represent the data of [9]. In this temperature range the curves of c_P are exactly the same of those of c_v translated vertically by the quantity R_{H_2}.

2.5.3 Sound speed

The sound speed is defined in terms of the pressure equation of state as follows:

$$[c(T,v)]^2 = \left(\frac{\partial P}{\partial \rho}\right)_s = v^2 \left[\frac{T}{c_v(T,v)}\left(\frac{\partial P}{\partial T}\right)_v^2 - \left(\frac{\partial P}{\partial v}\right)_T\right].$$

A simple calculation gives, in dimensionless form:

$$\frac{[c(t,v)]^2}{R_{\mathrm{H}_2} T_{\mathrm{v}}} = \left[\frac{(1+\alpha+t\alpha_t)^2}{c_v(t,v)/R_{\mathrm{H}_2}} + 1 + \alpha - v\alpha_v\right] t. \tag{2.16}$$

Figure 4 shows the behaviour of the sound speed computed using (2.16), for different values of the specific volume.

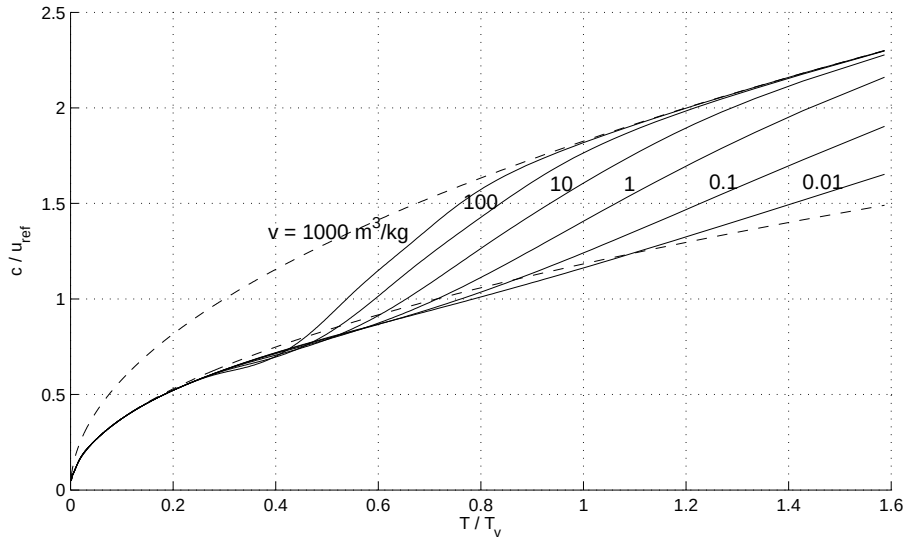

Figure 4: Adimensional sound speed $c(T,v)/\sqrt{R_{\mathrm{H}_2} T_{\mathrm{v}}}$ (solid), for different values of the specific volume. The dashed curves represent the sound speed of monatomic ideal gas (upper) and diatomic undissociated ideal gas (lower).

2.5.4 Fundamental derivative of gasdynamics

The fundamental derivative of gasdynamics, introduced by Thompson [12], is of primary importance in the definition of the nonlinearity characteristics of the Euler equations, as discussed in sections 4.2 and 4.5. By definition, the fundamental derivative of gasdynamics is:

$$\Gamma = 1 - \frac{v}{c}\frac{\partial \tilde{c}(s,v)}{\partial v}.$$

The derivative of the sound speed function $c = \tilde{c}(s,v)$ with respect to v can be determined in terms of those of the available function $c = c(T,v)$ by reminding that $\tilde{c}(s,v) = c(T(s,v),v)$ and by employing the chain rule, to give

$$\left(\frac{\partial \tilde{c}}{\partial v}\right)_s = \frac{\partial c(T(s,v),v)}{\partial v} = \left(\frac{\partial c}{\partial T}\right)_v \left(\frac{\partial T}{\partial v}\right)_s + \left(\frac{\partial c}{\partial v}\right)_{T=T(s,v)}.$$

The partial derivative of T at constant entropy is evaluated by the implicit differentiation theorem which gives

$$\left(\frac{\partial \tilde{c}}{\partial v}\right)_s = -\left(\frac{\partial c}{\partial T}\right)_v \left(\frac{\partial s}{\partial v}\right)_T \Big/ \left(\frac{\partial s}{\partial T}\right)_v + \left(\frac{\partial c}{\partial v}\right)_T.$$

For the gas to behave in a classical way, i.e. compressive shock waves and undercompressive rarefaction waves, $\Gamma > 0$ is required. This condition is always verified for the hydrogen gas in the dissociation region, as shown in figure 5. Since $\Gamma > 1$ for the range of temperatures and specific volume considered, the sound speed increases with pressure, as argued in [12].

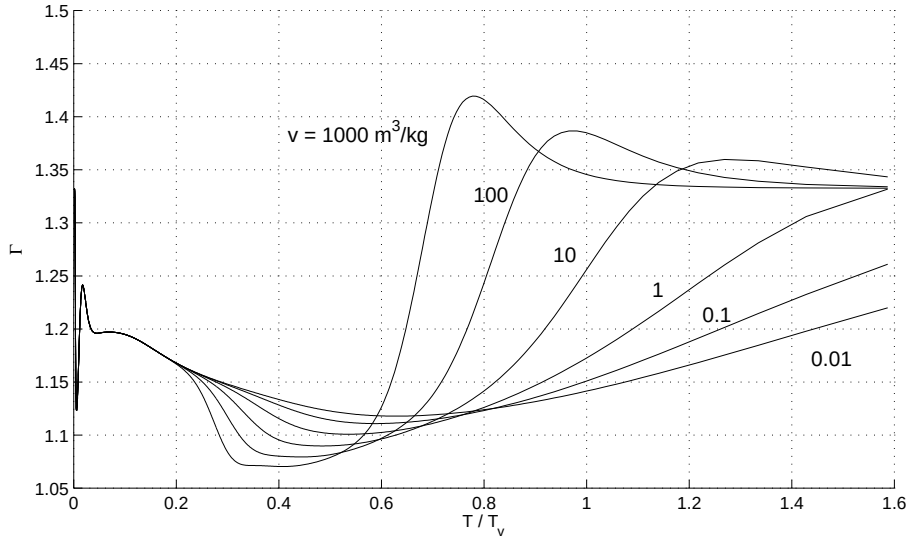

Figure 5: Fundamental derivative of gasdynamics $\Gamma(T,v)$, for different values of the specific volume.

3 Simplified hydrogen model

In this chapter a simplified thermodynamic model for a dissociating diatomic ideal gas is described. Differently from chapter 2, rotations are now taken as fully excited and completely uncoupled from vibrations which are instead still represented through the Morse potential. Thus, equation (A.14) will be used to express the partition function of the hydrogen molecule H_2, whereas for the atom H the expression remains the same of the previous model (equation (A.16)).

Following the same steps of the previous chapter, we will derive expressions for the equations of state for energy, entropy and other relevant thermodynamic properties of the gas. In order to underline the differences resulting from different treatment of rotations, this simplified model will be compared with the previous one. A further comparison will be made with a chemical model (HC) of the mixture H–H_2 based on the *law of mass action*.

3.1 Dissociation equation and equilibrium properties

Dissociation equation

Using the stationarity of the Helmholtz free energy and the conservation of the atomic constituents of the gas leads to:

$$\frac{\alpha^2}{1-\alpha} = \frac{\sqrt{t}\,\mathrm{e}^{-t_\mathrm{d}/t}}{z(t)}\frac{v}{v_\mathrm{d}} \equiv B(t,v), \tag{3.1}$$

where $z(t) = \mathrm{e}^{-De/k_\mathrm{B}T} Z_\mathrm{v}(T)$ with $Z_\mathrm{v}(T)$ the vibrational partition function (A.10) and we have introduced the constant:

$$\frac{1}{v_\mathrm{d}} = \frac{(g^0_\mathrm{H})^2 H^{5/2}}{2\sqrt{2}\, g^0_{\mathrm{H}_2}} T_\mathrm{r}\sqrt{T_\mathrm{v}}\frac{(2\pi k_\mathrm{B})^{3/2} u^{5/2}}{h^3}.$$

As a consequence, the dissociation coefficient is again uniquely determined by (3.1) as a function of t and v, so that at equilibrium $\alpha = \alpha(t,v)$:

$$\alpha(t,v) = \frac{1}{2}B(t,v)\left[\sqrt{1+4/B(t,v)}-1\right]. \tag{3.2}$$

Energy and entropy equations of state

Using the definitions of the internal energy (2.7) and entropy (2.9), the fundamental relation can be expressed in the parametric form:

$$\begin{cases} \epsilon(t,v) = \dfrac{1}{2}(5+\alpha)t + (1-\alpha)[\epsilon_{\mathrm{v}}(t) - t_{\mathrm{d}}], \\ \sigma(t,v) = \dfrac{1}{2}(5+\alpha)(1+\ln t) + (1-\alpha)\sigma_{\mathrm{v}}(t) \\ \qquad\qquad + (1+\alpha)\left[1 + \ln\left(\dfrac{v}{v_{\mathrm{d}}}\right)\right] + \Upsilon(\alpha) + \sigma_0, \end{cases} \tag{3.3}$$

where $\epsilon_{\mathrm{v}}(t) = x(t)/z(t)$ with $x(t) = z'(t)\,t^2$ and $\sigma_{\mathrm{v}}(t) = \frac{x(t)}{t\,z(t)} + \ln z(t)$ denote the contributions to the internal energy and entropy due to vibrations, while $\Upsilon(\alpha) = -2\alpha\ln\alpha - (1-\alpha)\ln(1-\alpha)$ is the contribution to the entropy due to the mixing of the molecular and atomic species and σ_0 represents the entropy in a reference state.

Pressure

The pressure function and its derivatives with respect to t and v are exactly the same introduced in chapter 2 with α given by the equation (3.1).

Specific heats

Starting from their definitions we obtain, in adimensional form:

$$\begin{aligned} \frac{c_v(t,v)}{R_{\mathrm{H_2}}} &= \frac{1}{2}(5+\alpha) + (1-\alpha)\epsilon_{\mathrm{v}}'(t) + \left[\frac{t}{2} - [\epsilon_{\mathrm{v}}(t) - t_{\mathrm{d}}]\right]\alpha_t, \\ \frac{c_P(t,v)}{R_{\mathrm{H_2}}} &= c_v(t,v) + \frac{(1+\alpha+t\,\alpha_t)^2}{1+\alpha-v\,\alpha_v}. \end{aligned} \tag{3.4}$$

Sound speed and fundamental derivative of gasdynamics

As for the pressure, the sound speed and the fundamental derivative of gasdynamics are the same introduced in chapter 2, with α given by equation (3.1) and c_v by equation (3.4).

3.2 Comparison between the models

The comparison of the *roto-vibra dissociating* (RVD) model of chapter 2 with the *vibra dissociating* (VD) model just described, shows how the different treatment of rotations affects the thermodynamics of the gas.

First, the dissociation coefficient $\alpha(t, v)$ is analyzed. Figure 6 shows the comparison between RVD and VD models for different values of the specific volume v. The RVD model gives always a lower value of α. When the gas is very diluted (high values of v), relative differences are small (below 5%) and the two models give almost the same value of α. As the specific volume decreases, differences become more important: for $v = 0.01$ m^3/kg they reach about 13%. This will have an impact on some of the other properties, as we can see in the next figures.

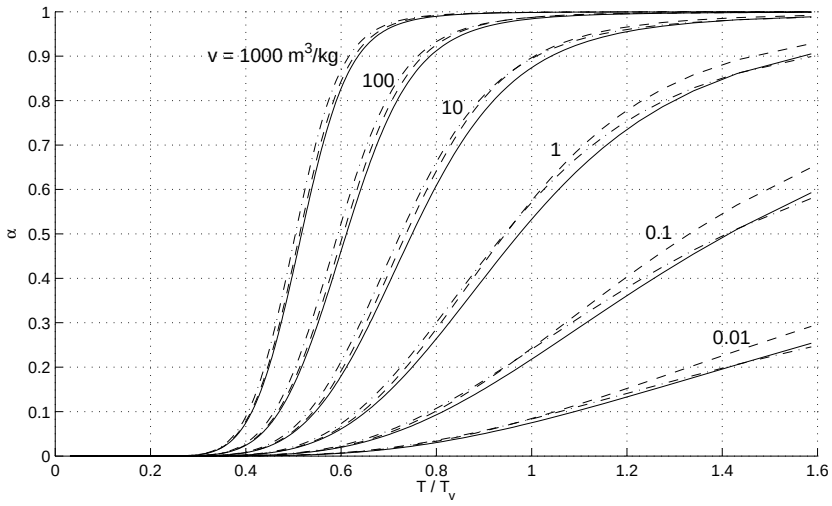

Figure 6: Dissociation coefficient $\alpha(t, v)$ for the RVD (solid), VD (dashed) and HC model (dashed-dotted), for different values of the specific volume.

Despite differences in the dissociation coefficient, the values of the pressure computed from equation (2.12), with α respectively obtained from (2.5) and (3.1), are extremely close. Maximum differences increase with $1/v$ but are always below 4% in the range of specific volumes and temperature analyzed.

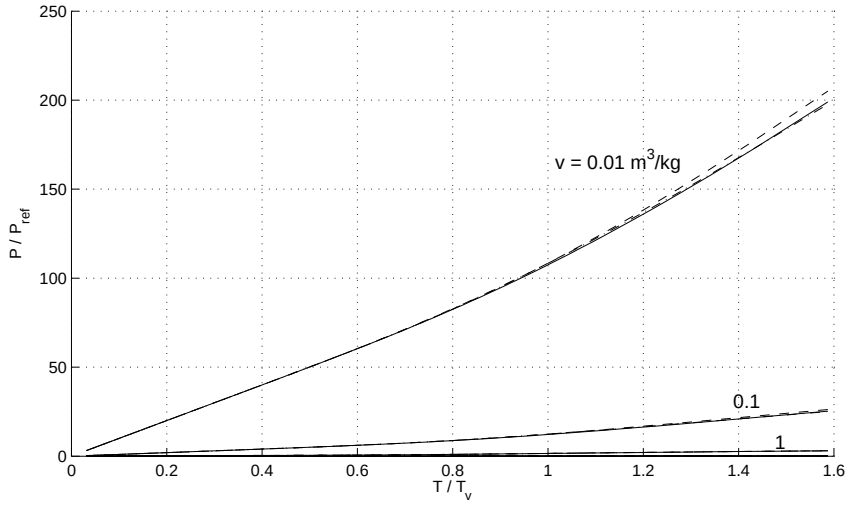

Figure 7: Adimensional pressure for the RVD (solid), VD (dashed) and HC model (dashed-dotted), for different values of the specific volume.

The most important differences are found to be in the specific heats. Similarly to the other thermodynamic properties, differences between the two models increase with $1/v$, reaching about 10% near the peaks. Furthermore, a completely different behaviour is found in the low temperature region. As we can see in figure 9, the specific heat c_v given by the VD model has a starting value of $c_v = \frac{5}{2}R_{\mathrm{H}_2}$, since rotations are considered as fully excited and their contribution to the specific heat is constant $c_v^{\mathrm{rot}} = R_{\mathrm{H}_2}$. On the contrary, the RVD model considers the transient between the unexcited and the fully excited rotations, leading to very different values of c_v for low temperatures. In this region the differences can reach about 40%, making mandatory the RVD model to properly describe the behaviour of the gas. For the specific heat c_P the comments are exactly the same.

If we analyze the ratio of the specific heats $\gamma = c_P/c_v$, we find that, except for very small values of temperature, the differences between the two models weaken and are $< 2\%$ in the range of temperatures and specific volumes considered.

The last thermodynamic properties compared are the sound speed and the fundamental derivative of gasdynamics, for which differences are found to be $< 2\%$ in both cases, establishing a substantial equivalence between the two models.

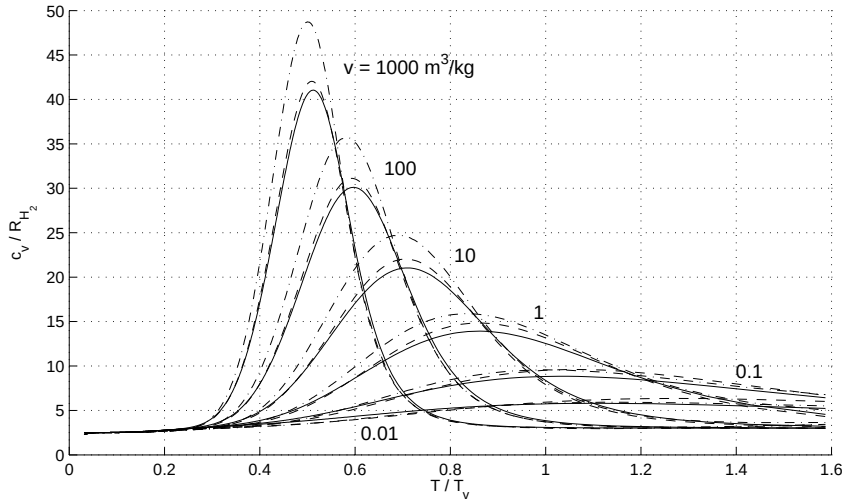

Figure 8: Specific heat c_v for the RVD (solid), VD (dashed) and HC model (dashed-dotted), for different values of the specific volume.

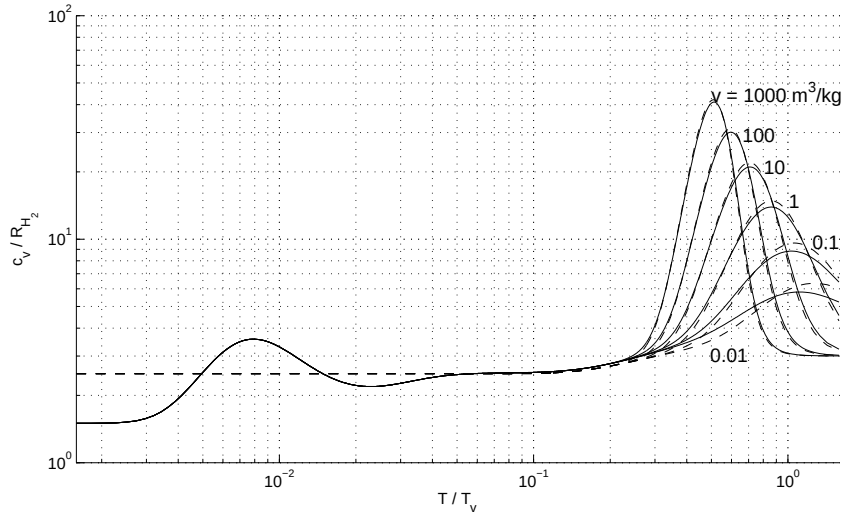

Figure 9: Adimensional specific heat c_v in logarithmic scale for both RVD model (solid) and VD model (dashed), for different values of the specific volume.

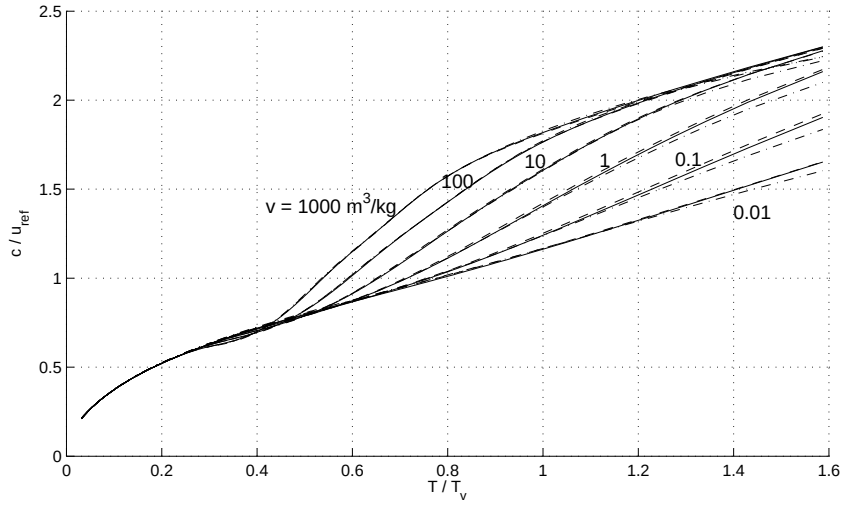

Figure 10: Adimensional sound speed for the RVD (solid), VD (dashed) and HC model (dashed-dotted), for different values of the specific volume.

Before we proceed with the analysis of the Riemann problem for the hydrogen gas, it is useful to compare the results obtained through the RVD and VD model with a very simple gas model which considers classic rigid rotations, harmonic vibrations and uses the law of mass action in order to determine the equilibrium composition of the mixture. We will refer to this model as HC model (*harmonic-chemical*). Descriptions of this model can be found in many gasdynamics text books, see for example [13, 14].

Figures 6, 7, 8 and 10 show comparisons between the three models on four representative thermodynamic properties. The HC model overestimates the value of the specific heat c_v, moreover it gives higher values of the dissociation coefficient for most values of v analyzed. Differences on α between the HC model and the RVD model are about 15% –20% with $2500 < T < 5000$. They reach almost 30% on c_v near its peak for the most diluted gas and 10% for $v = 0.01$ m^3/kg. The accord between the models is more satisfying with regard to the sound speed and pressure, with differences $< 5\%$ in both cases.

4 Riemann problem for dissociating gas

In this chapter the Riemann problem of gasdynamics will be analyzed. It is an initial value problem for the system of Euler equations with particular initial conditions. The variables are characterized by a jump in their initial values, and are uniform on the left side and on the right side of a discontinuity; the two different states will be referred to as the *left state* and the *right state*. Since there is no reference length in the problem statement, the solution is self similar, namely it is constant along any ray of the *x-t* plane. In general the solution consists of three waves: *shock* or *rarefaction waves* and *contact discontinuity*, possibly of vanishing intensity. The intermediate wave is always a contact discontinuity while each of the two external waves can be either a shock or a rarefaction wave depending on the initial conditions. The solution of the Riemann problem is very important in the simulation of compressible flows since the Riemann problem is the starting point to formulate *finite volume methods* where it is solved at every interface between two grid cells and at every time level.

Following Quartapelle et al. [4], we will first analyze the eigenstructure of the Euler equations which leads to the determination of the mathematical and physical nature of the three different waves. Then a suitable formulation of the equations which describe the shock and the rarefaction wave for the case of the dissociating gas will be introduced and the solution technique will be presented.

4.1 Eigenstructure of Euler equations

The Riemann problem of gasdynamics is formulated starting from the Euler equations written in quasi-linear form and with the energy balance equation replaced by the entropy transport equation under the assumption that any dissipative phenomena can be disregarded. The resulting system of hyperbolic equations of gasdynamics assumes the form:

$$\frac{\partial \mathbf{w}}{\partial t} + \mathbf{A}(\mathbf{w}) \frac{\partial \mathbf{w}}{\partial x} = 0$$

with vector $\mathbf{w}$ and matrix $\mathbf{A}(\mathbf{w})$ defined as follows:

$$\mathbf{w} = \begin{pmatrix} v \\ u \\ s \end{pmatrix} \quad \text{and} \quad \mathbf{A}(\mathbf{w}) = \begin{pmatrix} u & -v & 0 \\ v\left(\frac{\partial P}{\partial v}\right)_s & u & v\left(\frac{\partial P}{\partial s}\right)_v \\ 0 & 0 & u \end{pmatrix}.$$

Here v denotes the specific volume, u the velocity, s the specific entropy and $P = P(s, v)$ is the pressure equation of state of the gas considered. The eigenvalues of $\mathbf{A}(\mathbf{w})$ represent the speed at which information travels in the fluid and are the eigenvalues of the characteristic equation:

$$|\mathbf{A}(\mathbf{w}) - \lambda(\mathbf{w})\mathbf{I}| = 0.$$

which gives:

$$\lambda_1(\mathbf{w}) = u - c(s, v), \qquad \lambda_2(\mathbf{w}) = u, \qquad \lambda_3(\mathbf{w}) = u + c(s, v),$$

with $c(s, v) = [\partial P(s, \rho)/\partial\rho]^{1/2}$ denoting the sound speed of the fluid. These eigenvalues are indipendent from the choice of the variables used to formulate the Euler system: using for example the density ρ instead of the specific volume v would have led to exactly the same values of λ_i.

To understand the nonlinear nature of the Euler system we have to compute the eigenvectors associated with the three eigenvalues. The eigenvectors are easily found to be:

$$\mathbf{r}_1(\mathbf{w}) = \begin{pmatrix} v \\ c(s, v) \\ 0 \end{pmatrix}, \quad \mathbf{r}_2(\mathbf{w}) = \begin{pmatrix} -\left(\frac{\partial P}{\partial s}\right)_v \\ 0 \\ \left(\frac{\partial P}{\partial v}\right)_s \end{pmatrix}, \quad \mathbf{r}_3(\mathbf{w}) = \begin{pmatrix} v \\ -c(s, v) \\ 0 \end{pmatrix}.$$

4.2 Linear degeneracy and genuine nonlinearity

Every eigenvalue $\lambda_i(\mathbf{w})$ defines a scalar field in the space of vectors $\mathbf{w} = (v, u, s)^{\mathrm{T}}$ and every eigenvector $\mathbf{r}_i(\mathbf{w})$ defines a vector field in the same three-dimensional space. At the same time, the gradient of the eigenvalue $\boldsymbol{\nabla}_{\mathbf{w}}\lambda_i(\mathbf{w})$ defines another vector field. The linear or nonlinear nature of the wave associated to each eigenvalue depends on a simple geometrical relationship between the field of the eigenvector and that of the gradient of the corresponding eigenvalue, expressed by the scalar product $\mathbf{r}(\mathbf{w}) \cdot \boldsymbol{\nabla}_{\mathbf{w}}\lambda(\mathbf{w})$. If this product never vanishes, then the eigenvalue is said to be *genuinely nonlinear* while if it is always zero than the eigenvalue is *linearly degenerate*. For the Euler equations we can observe that the second eigenvalue is always linearly degenerate and that the first and third eigenvalues are found to be such that:

$$\mathbf{r}_1(\mathbf{w}) \cdot \boldsymbol{\nabla}_{\mathbf{w}}\lambda_1(\mathbf{w}) = c\Gamma \qquad \text{and} \qquad \mathbf{r}_3(\mathbf{w}) \cdot \boldsymbol{\nabla}_{\mathbf{w}}\lambda_3(\mathbf{w}) = -c\Gamma,$$

where Γ is the fundamental derivative of gasdynamics. As already shown in chapter 2, the function Γ never vanishes for the gas considered here.

4.3 Contact discontinuity

We first analyze the contact discontinuity. Let us consider a wave travelling at a speed given by the second eigenvalue of the Euler equations and determine the change of the variables inside such a wave. This means to find the vector function $\mathbf{w} = \mathbf{w}(q)$ solution to the ordinary differential system:

$$\frac{d\mathbf{w}}{dq} = \alpha(q)\, \mathbf{r}_2(\mathbf{w}),$$

with q a parameter which represents the indipendent variable and $\alpha(q)$ an arbitrary function whose choice fixes a parameterization of the solution. In terms of the components of $\mathbf{r}_2(\mathbf{w})$, we have:

$$\begin{cases} \dfrac{dv}{dq} = -\alpha(q)\, \dfrac{\partial P(s,v)}{\partial s}, \\ \dfrac{du}{dq} = 0, \\ \dfrac{ds}{dq} = \alpha(q)\, \dfrac{\partial P(s,v)}{\partial v}. \end{cases}$$

So, the velocity is constant through the contact discontinuity. Moreover, the ratio of the first and third equations gives

$$\frac{dv}{ds} = -\frac{\partial P(s,v)}{\partial s} \Big/ \frac{\partial P(s,v)}{\partial v}.$$

Let us now define a function of three independent variables:

$$\Phi(s,v,P) \equiv P(s,v) - P,$$

so that the equation $\Phi(s,v,P) = 0$ implicitly defines a function $v = v(s,P)$. The derivative of $v(s,P)$ with respect to entropy is obtained by means of the theorem of partial derivation of the implicit functions:

$$\left(\frac{\partial v}{\partial s}\right)_P = -\frac{\dfrac{\partial \Phi(s,v,P)}{\partial s}}{\dfrac{\partial \Phi(s,v,P)}{\partial v}} = -\frac{\dfrac{\partial P(s,v)}{\partial s}}{\dfrac{\partial P(s,v)}{\partial v}}.$$

Since this expression coincides with dv/ds along the contact discontinuity, the pressure is constant along the wave considered, whereas v and any other thermodynamic variable different from pressure can experience a jump in its values.

To summarize, the characteristic of the contact discontinuity is the constancy of both velocity and pressure; as we will see, these conditions will be used to formulate the Riemann problem as a system of two nonlinear equations with unknowns the values of the temperature on both sides of the wave.

4.4 Rarefaction wave

We now analyze the rarefaction wave. Let us consider a wave linking a given initial state $(v_i, u_i, s_i)^{\mathrm{T}}$ with the states belonging to the *integral curves*, which are by definition the curves tangent in every point to the direction of a given eigenvector. In other words, an integral curve is the solution of the ordinary differential equations system

$$\frac{d\mathbf{w}}{dq} = \alpha(q)\,\mathbf{r}_{1|3}(\mathbf{w}),$$

with initial condition $\mathbf{w}(0) = \mathbf{w}_i = (v_i, u_i, s_i)^{\mathrm{T}}$. For genuinely nonlinear eigenvectors, it is possible to use the eigenvalue as the parameter $q = \xi = \lambda_{1|3}(\mathbf{w}(\xi))$ of the curve. The derivative of this relation with respect to ξ gives $\alpha(\xi) = \pm 1/[c(s,v)\,\Gamma(s,v)]$. The system becomes:

$$\frac{d\mathbf{w}}{d\xi} = \frac{\pm\mathbf{r}_{1|3}(\mathbf{w})}{c(s,v)\,\Gamma(s,v)}, \tag{4.1}$$

and must be solved with the initial condition $\mathbf{w}(\xi_i) = \mathbf{w}_i$, with $\xi_i = \lambda_{1|3}(\mathbf{w}_i)$. Substituting the expression of $\mathbf{r}_{1|3}(\mathbf{w})$, the equation of the third component of (4.1) says that the rarefaction wave is isentropic.

Reminding the thermodynamic models introduced in chapters 2 and 3, we can write in dimensionless form:

$$\sigma^{\mathrm{f}}(t, v, \alpha(t,v)) = \sigma_i,$$

where $\sigma_i = \sigma^{\mathrm{f}}(t_i, v_i, \alpha_i)$ and α_i the solution of $\alpha_i^2 + \beta(t_i, v_i)(\alpha_i - 1) = 0$. The determination of the isentropic trasformation of the gas with specific entropy σ_i requires to solve a nonlinear system of two equations:

$$\begin{cases} \phi(t, v, \alpha, \sigma_i) = \sigma^{\mathrm{f}}(t, v, \alpha) - \sigma_i = 0 \\ \psi(t, v, \alpha) = \alpha^2 + \beta(t, v)(\alpha - 1) = 0 \end{cases} \tag{4.2}$$

which, for any fixed t, gives the solution $v = v^{\mathrm{rar}}(t, \sigma_i)$ and $\alpha = \alpha^{\mathrm{rar}}(t, \sigma_i)$ along the isentrope passing through (t_i, v_i). Thus, the solution of the rarefaction wave for the case of the dissociating gas is more complicated than for the polytropic ideal gas and requires the solution of the system (4.2) by means of the Newton method. The pressure is provided immediately by the equation of state:

$$P^{\mathrm{rar}}(T; \mathbf{i}) = P(T, v^{\mathrm{rar}}(T, \sigma_i)).$$

The system (4.1) is reduced to only two equations and it is possible to obtain a direct relationship between velocity and specific volume by taking the ratio between the

two first equations. The first order differential equation is separable and can be integrated to obtain:

$$u_{1|3}^{\text{rar}}(v;\mathbf{i}) = u_i \pm \int_{v_i}^{v} \frac{c(s_i,v')}{v'}\,dv'.$$

As we have seen in the description of the thermodynamics of the dissociating hydrogen gas, the most convenient independent variable used to define all the other properties is the temperature. So, taken T as the independent variable, we have:

$$\begin{aligned} P^{\text{rar}}(T;\mathbf{i}) &= P(s_i,T),\\ u_{1|3}^{\text{rar}}(T;\mathbf{i}) &= u_i \pm \int_{T_i}^{T} \frac{c(s_i,T')}{v^{\text{rar}}(T';\mathbf{i})}\frac{dv^{\text{rar}}(T';\mathbf{i})}{dT'}\,dT'. \end{aligned} \tag{4.3}$$

The derivative dv^{rar}/dT can be evaluated by using the differentiation rule for implicit functions:

$$\frac{dv^{\text{rar}}}{dT} = -\frac{\dfrac{\partial(\phi,\psi)}{\partial(T,\alpha)}}{\dfrac{\partial(\phi,\psi)}{\partial(v,\alpha)}} = -\frac{\dfrac{\partial\phi}{\partial T}\dfrac{\partial\psi}{\partial\alpha} - \dfrac{\partial\phi}{\partial\alpha}\dfrac{\partial\psi}{\partial T}}{\dfrac{\partial\phi}{\partial v}\dfrac{\partial\psi}{\partial\alpha} - \dfrac{\partial\phi}{\partial\alpha}\dfrac{\partial\psi}{\partial v}}. \tag{4.4}$$

Finally, we must notice that, when the solution of the Riemann problem consists of two rarefaction waves, for particular values of the initial velocities it is possible the formation of a region of vacuum behind the wave's tails. This circumstance is identified by the vanishing of the temperature on the contact discontinuity. We can define a relative velocity ν_{vacuum}:

$$\nu_{\text{vacuum}} = -\int_0^{T_\ell} \frac{c(s_\ell,T)}{v^{\text{rar}}(T;\mathbf{l})}\frac{dv^{\text{rar}}(T;\mathbf{l})}{dT}\,dT - \int_0^{T_r} \frac{c(s_r,T)}{v^{\text{rar}}(T;\mathbf{r})}\frac{dv^{\text{rar}}(T;\mathbf{r})}{dT}\,dT \tag{4.5}$$

such that, for $\nu_{r\ell} = u_r - u_\ell \geq \nu_{\text{vacuum}}$, a region of vacuum occurs.

4.5 Shock wave

In this section the solution of the shock wave is obtained. In general the shock moves with a speed $\sigma \neq 0$ with respect to the system of reference in which the Riemann problem is defined. The solution is achieved using the Rankine–Hugoniot jump conditions $\mathbf{f}(\mathbf{w}) - \mathbf{f}(\mathbf{w}_i) = \sigma[\mathbf{w} - \mathbf{w}_i]$, with $\mathbf{f}(\mathbf{w})$ the flux of the hyperbolic system in the conservative form and $\mathbf{w} = (\rho, m = \rho u, E^{\text{t}})^{\text{T}}$. It

is convenient to move to the frame of reference of the shock in which the fluid velocity is $U = u - \sigma$, so that a steady-state version of the Rankine–Hugoniot conditions is obtained, namely:

$$\begin{cases} U_i/v_i = U/v, \\ U_i^2/v_i + P_i = U^2/v + P, \\ \frac{1}{2}U_i^2 + e_i + P_i v_i = \frac{1}{2}U^2 + e + Pv. \end{cases}$$

Combining the three equations leads to the purely thermodynamic relation:

$$e(P, v) - e_i + \tfrac{1}{2}(P_i + P)(v - v_i) = 0,$$

which defines $P = P^{\mathrm{RH}}(v; \mathbf{i})$ implicitly.

Using the definition of the *mass velocity* $J = \dfrac{u - u_i}{v - v_i}$, it is possible to obtain the expression of the velocity behind the shock

$$u_{1|3}^{\mathrm{RH}}(v; \mathbf{i}) = u_i \mp \sqrt{-\big[P^{\mathrm{RH}}(v; \mathbf{i}) - P_i\big](v - v_i)}$$

in which the subscript $_{1|3}$ refers to the first and third eigenvalue of the Euler equations and the signs $\mp$ are determined by the property $\Gamma > 0$ which guarantees that the wave is compressive.

Similarly to the rarefaction wave, it is convenient to formulate the solution of the shock wave in terms of the temperature. Reminding the thermodynamic relations of the dissociating gas, the Rankine–Hugoniot equation becomes, in dimensionless form:

$$\epsilon^{\mathrm{f}}(t, \alpha) - \epsilon_i + \tfrac{1}{2}\big[p_i + p^{\mathrm{f}}(t, v, \alpha)\big](v - v_i) = 0,$$

were $\epsilon_i = \epsilon^{\mathrm{f}}(t_i, \alpha_i)$, $p_i = p^{\mathrm{f}}(t_i, v_i, \alpha_i)$ and α_i the solution of $\alpha_i^2 + \beta(t_i, v_i)(\alpha_i - 1) = 0$. The determination of the solution of the shock wave requires to solve a nonlinear system of two equations:

$$\begin{cases} \phi(t, v, \alpha, \sigma_i) = \epsilon^{\mathrm{f}}(t, \alpha) - \epsilon_i + \frac{1}{2}\big[p_i + p^{\mathrm{f}}(t, v, \alpha)\big](v - v_i) = 0, \\ \psi(t, v, \alpha) = \alpha^2 + \beta(t, v)(\alpha - 1) = 0, \end{cases} \tag{4.6}$$

which, for any fixed t, gives the solution $v^{\mathrm{RH}} = v(t; \mathbf{i})$ and $\alpha = \alpha(t; \mathbf{i})$ behind the shock. The pressure is provided immediately by the equation of state:

$$P^{\mathrm{RH}}(T; \mathbf{i}) = P(T, v^{\mathrm{RH}}(T; \mathbf{i})). \tag{4.7}$$

Now the velocity after the shock wave is easily expressed in the form

$$u_{1|3}^{\mathrm{RH}}(T;\mathbf{i}) = u_i \mp \sqrt{-\left[P^{\mathrm{RH}}(T;\mathbf{i}) - P_i\right]\left[v^{\mathrm{RH}}(T;\mathbf{i}) - v_i\right]}\,. \tag{4.8}$$

The derivative dv^{RH}/dT can be evaluated by using the differentiation rule for implicit functions:

$$\frac{dv^{\mathrm{RH}}}{dT} = -\frac{\dfrac{\partial\phi}{\partial T}\dfrac{\partial\psi}{\partial\alpha} - \dfrac{\partial\phi}{\partial\alpha}\dfrac{\partial\psi}{\partial T}}{\dfrac{\partial\phi}{\partial v}\dfrac{\partial\psi}{\partial\alpha} - \dfrac{\partial\phi}{\partial\alpha}\dfrac{\partial\psi}{\partial v}}. \tag{4.9}$$

4.6 Structure of the Riemann problem

Finally, the characteristics of the contact discontinuity described in section 4.3 can be exploited to formulate the equations representing the Riemann problem.

We will denote by $u_1(T;\mathbf{l})$ and $P(T;\mathbf{l})$ respectively the velocity and the pressure after the wave which connects the left state $\mathbf{l} = (T_\ell, P_\ell, u_\ell)^{\mathrm{T}}$ with a generic state characterized by a temperature T. The analytical form of the two functions $u = u_1(T;\mathbf{l})$ and $P = P(T;\mathbf{l})$ depends on the nature of the wave that can be either a shock wave ($T > T_\ell$) or a rarefaction wave ($T < T_\ell$). Similarly, $u_3(T;\mathbf{r})$ and $P(T;\mathbf{r})$ denote respectively the velocity and the pressure after the wave which connects the right state $\mathbf{r} = (T_r, P_r, u_r)^{\mathrm{T}}$ with a generic state characterized by a temperature T. We can summarize the form of $u_1(T;\mathbf{l})$ and $u_3(T;\mathbf{r})$ as follows:

$$u_1(v;\mathbf{l}) \equiv \begin{cases} u_1^{\mathrm{rar}}(T;\mathbf{l}) & \text{if } T < T_\ell \\ u_1^{\mathrm{RH}}(T;\mathbf{l}) & \text{if } T > T_\ell \end{cases} \quad \text{and} \quad u_3(v;\mathbf{r}) \equiv \begin{cases} u_3^{\mathrm{rar}}(T;\mathbf{r}) & \text{if } T < T_r \\ u_3^{\mathrm{RH}}(T;\mathbf{r}) & \text{if } T > T_r \end{cases}$$

with the superscripts $^{\mathrm{rar}}$ and $^{\mathrm{RH}}$ denoting the solution of the rarefaction wave or the shock wave given by equations (4.3) and (4.8). As already seen, the functions defining the velocities depend on the eigenvalues 1 and 3. Conversely, the functions defining the pressure are indipendent from the eigenvalue and are:

$$P(v;\mathbf{l}) \equiv \begin{cases} P^{\mathrm{rar}}(v;\mathbf{l}) & \text{if } T < T_\ell \\ P^{\mathrm{RH}}(v;\mathbf{l}) & \text{if } T > T_\ell \end{cases} \quad \text{and} \quad P(v;\mathbf{r}) \equiv \begin{cases} P^{\mathrm{rar}}(v;\mathbf{r}) & \text{if } T < T_r \\ P^{\mathrm{RH}}(v;\mathbf{r}) & \text{if } T > T_r \end{cases}$$

with P^{rar} and P^{RH} given by equations (4.3) and (4.7) respectively. To solve the Riemann problem requires to determine the values $T_\ell^\star$, $T_r^\star$, $P^\star$ and $u^\star$ which characterize the states on the two sides of the contact discontinuity. To simplify the notation we will refer to the two unknowns as $T \equiv T_\ell^\star$ and $W \equiv T_r^\star$. To guarantee

the property of equality of the values of velocity and pressure on the two sides of the contact discontinuity, T and W must be the solutions of the nonlinear system of two equations:

$$\begin{cases} u_1(T;\mathbf{l}) = u_3(W;\mathbf{r}), \\ P(T;\mathbf{l}) = P(W;\mathbf{r}), \end{cases}$$

which can be written also as:

$$\begin{cases} \phi_{(\ell,r)}(T,W) = 0, \\ \psi_{(\ell,r)}(T,W) = 0, \end{cases}$$

where $\phi_{(\ell,r)}(T,W) = u_1(T;\mathbf{l}) - u_3(W;\mathbf{r})$ and $\psi_{(\ell,r)}(T,W) = P(T;\mathbf{l}) - P(W;\mathbf{r})$. This system can be solved numerically with a Newton method, which needs to evaluate the Jacobian matrix:

$$\frac{\partial(\phi_{(\ell,r)},\psi_{(\ell,r)})}{\partial(T,W)} \equiv \begin{pmatrix} \dfrac{du_1(T;\mathbf{l})}{dT} & -\dfrac{du_3(W;\mathbf{r})}{dW} \\ \dfrac{dP(T;\mathbf{l})}{dT} & -\dfrac{dP(W;\mathbf{r})}{dW} \end{pmatrix}. \tag{4.10}$$

For the case of the gas considered [2], the expressions of the elements of the Jacobian matrix, when the wave is a rarefaction wave, are the following:

$$\frac{du_{1|3}^{\text{rar}}(T;\mathbf{i})}{dT} = \pm\frac{c(s_i,T)}{v^{\text{rar}}(T;\mathbf{i})}\frac{dv^{\text{rar}}(T;\mathbf{i})}{dT}$$

and

$$\frac{dP^{\text{rar}}(T;\mathbf{i})}{dT} = \frac{dP(T,v^{\text{rar}}(T;\mathbf{i}))}{dT} = \frac{\partial P(T,v)}{\partial T} + \frac{\partial P(T,v)}{\partial v}\frac{dv^{\text{rar}}(T;\mathbf{i})}{dT}.$$

The derivative $dv^{\text{rar}}(T;\mathbf{i})/dT$ is given by equation (4.4). On the other hand, when the wave is a shock wave, the derivatives are:

$$\frac{dP^{\text{RH}}(T;\mathbf{i})}{dT} = \frac{dP(T,v^{\text{RH}}(T;\mathbf{i}))}{dT} = \frac{\partial P(T,v)}{\partial T} + \frac{\partial P(T,v)}{\partial v}\frac{dv^{\text{RH}}(T;\mathbf{i})}{dT}$$

and

$$\frac{du_{1|3}^{\text{RH}}(T;\mathbf{i})}{dT} = \pm\frac{\dfrac{dP^{\text{RH}}(T;\mathbf{i})}{dT}\left[v^{\text{RH}}(T;\mathbf{i}) - v_i\right] + \dfrac{dv^{\text{RH}}(T;\mathbf{i})}{dT}\left[P^{\text{RH}}(T;\mathbf{i}) - P_i\right]}{2\sqrt{-[P^{\text{RH}}(T;\mathbf{i}) - P_i][v^{\text{RH}}(T;\mathbf{i}) - v_i]}},$$

[2] As well as for any mixture of nonpolytropic gases.

where $dv^{\mathrm{RH}}(T;\mathbf{i})/dT$ is given by equation (4.9).

The existence and uniqueness of the solution of the Riemann problem can be demonstrated under the assumption that $\partial e(P,v)/\partial v > 0$. In this case the Newton method will converge to the solution provided the initial guess is close enough to the solution: taking the initial guess as the arithmetic mean of the two initial values T_ℓ and T_r is simple and turns out to be also effective.

5 Results

In this chapter the Hugoniot curves for the hydrogen gas are first analyzed to highlight the consequences of the dissociation. Then, results of some Riemann problem in the presence of dissociation and in the low temperature region are presented and discussed. Three different kinds of solutions are considered: symmetrical solutions with either two rarefaction waves or two shock waves, and mixed solutions with one rarefaction wave and one shock wave. A comparison between the results obtained by means of the RVD and VD models is made. Initial conditions for every Riemann problem are suggested by the analysis of chapter 3, in order to underline differences between the models for certain initial thermodynamic data, as well as to verify their equivalence for other initial data. Finally, for the case of the shock waves, a comparison with results provided in [5] is made.

5.1 Hugoniot curves

The *Hugoniot curve* or *Hugoniot adiabat* is fundamental in the study of shock waves. It is the locus of all the thermodynamic states (v, P) which may be connected by a single shock to an initial state (v_0, P_0).

Starting from a small value of pressure (and so of temperature), the Hugoniot curve first tends to the vertical asymptote pertaining to the diatomic undissociated ideal gas. When pressure increases further, dissociation occurrs and makes the curve cross the diatomic gas asymptote. Then, for higher pressures, the Hugoniot curve reaches a minimum value of v, after which the curve has an inversion when the dissociation is complete. Finally, the curve tends to the vertical asymptote of the monatomic gas, but from the left side instead of from the right. Figure 11 shows the adiabats for the RVD and VD model. They agree quite well, except for small values of the pressure after the shock. This will determine differences in the solution of the Riemann problem with two shock waves in the low temperature region. The dissociation coefficient α after the shock increases with the shock strength because the increment in temperature prevails over the diminishing specific volume.

Furthermore, referring to Bates and Montgomery [15], it is interesting to notice that, if the shock is strong enough, an exotic mechanism known as *acoustic emission* could manifests. This is a shock wave instability which does not imply an anomalous behaviour of the shock since Γ is always positive. It requires the slope of the Hugoniot curve to be within a critical range. Figure 11 confirms this occurrence for the hydrogen gas when the shock wave is such to connect an initial low temperature state to completely dissociated conditions. The analysis of this kind of instability is very important in the study of the implosion of *inertial confinement fusion of pellet materials*, for which the hydrogen is used. However, this

subject goes beyond the aim of this work, we just wanted to show that the criterion for such shock instability can be met when the shock is strong enough.

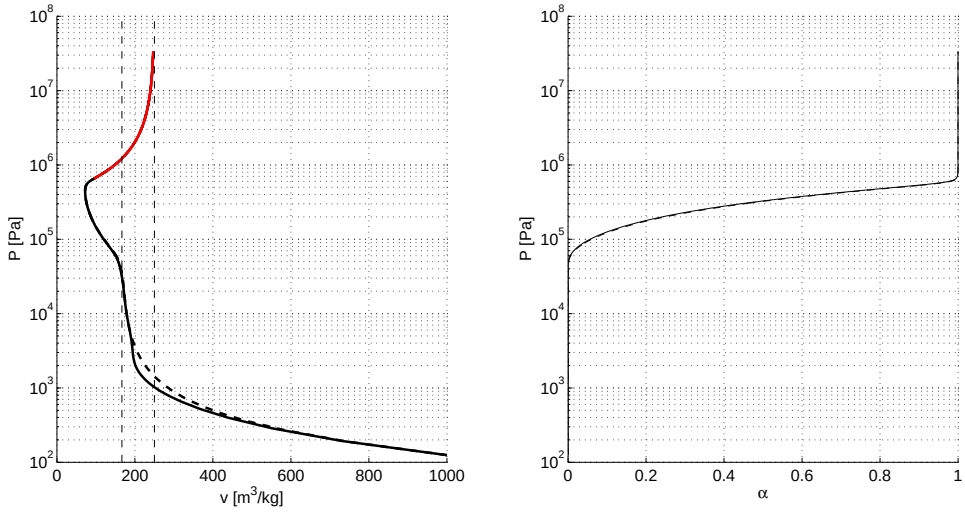

Figure 11: Left plot shows the Hugoniot curves for the RVD (solid) and VD (dashed) model. Curves become red when instability criterion is met. Vertical lines represent the asymptotes for the diatomic undissociated molecular gas (left) and the monatomic gas (right). Right plot shows the dissociation coefficient α after the shock. For both plot the initial state is $T_0 = 30\,\mathrm{K}$ and $v = 1000\,\mathrm{m}^3/\mathrm{kg}$.

5.2 Shock waves

To have a symmetrical solution made of two shock waves, equal thermodynamic conditions must be chosen initially on the two sides of the discontinuity, while the velocities must be opposite, positive on the left and negative on the right side. First, we focus on initial conditions which can generate the dissociation of the gas after the shock wave.

A wide interval of initial temperatures $500\,\mathrm{K} < T_0 < 7000\,\mathrm{K}$ and velocities in the range $1300\,\mathrm{m/s} < |u_0| < 23000\,\mathrm{m/s}$, for values of the specific volume $1\,\mathrm{m}^3/\mathrm{kg} < v_0 < 1000\,\mathrm{m}^3/\mathrm{kg}$, have been analyzed.

It is possible to make a comparison between the results obtained by means of the RVD and VD models. The analysis of chapter 3 shows very small differences on the thermodynamic properties when the mixture approaches one of the two limiting conditions of molecular and atomic gas, especially for large values of v.

Differences become more important when the ideal gas is only partially dissociated and relatively dense. These conditions have an impact on the solution of the Riemann problem. In fact, when the initial data are such that the gas is almost undissociated or reaches a high level of dissociation after the shock (near 90%), the solution of the Riemann problem provided by the two models are merely equal and the differences slightly exceed a few $\%$ on all the thermodynamic properties, showing a tendency to increase with $1/v$. When the shocks are strong enough to cause only a partial dissociation of the gas (about 10%–40%), the differences become more relevant on α, although they remain quite low on the other thermodynamic properties. Since two different thermodynamic models are used, it is impossible to guarantee the same initial values of P and α, for any fixed (T, v). It is interesting to notice that, in this region of partial dissociation, the initial difference of these quantities is almost conserved after the shock. The general agreement of the solutions is due to the very small differences found in the Hugoniot curves for the two models. Figure 12 shows the solution of the symmetrical Riemann problem with $T_0 = 6000\,\mathrm{K}$, $v_0 = 0.1\,\mathrm{m}^3/\mathrm{kg}$ and $u_0 = \pm 6140\,\mathrm{m/s}$. We can see the substantial agreement of the specific volume, pressure and temperature with differences all $< 1\%$. The difference on the value of α on the contact discontinuity exceeds 10%.

The results obtained by means of RVD and VD models can be compared with the data provided by NASA [5]. This reference employs a thermodynamic model assuming rigid rotations and harmonic vibrations of the molecules, with a correction to take into account the coupling between these two motions. The properties behind the shock are obtained through an iterative method. Two different values of the initial specific volume are taken into account and the speed of the moving shock u_s lies in the interval $4\,\mathrm{km/s} < u_\mathrm{s} < 24\,\mathrm{km/s}$. The thermodynamic properties of the gas behind the shock agree quite well with the reference data (with relative differences $< 5\%$), except for the composition of the mixture which differs by a quantity 15%–40%.

It is also interesting to study the solution of the Riemann problem for the hydrogen gas for $T < 150\,\mathrm{K}$, due to the relatively high value of its rotational temperature which spreads the transient between unexcited and fully excited rotations in a wider interval of temperatures and at higher values than for other diatomic molecules. The analysis of chapter 3 shows how the RVD and VD models determine a completely different behaviour of some thermodynamic properties of the gas, e.g. specific heats. Also the Hugoniot curves of figure 11 confirm substantial differences between the models. This has consequences on the solution of the Riemann problem in the low temperature region which shows relevant differences on pressure, specific volume and temperature on the contact discontinuity, respectively of 3%, 7% and 9%. Figure 13 shows the solution of the Riemann problem for $T_0 = 50\,\mathrm{K}$ and $u_0 = \pm 1000\,\mathrm{m/s}$. The value of the initial specific volume is

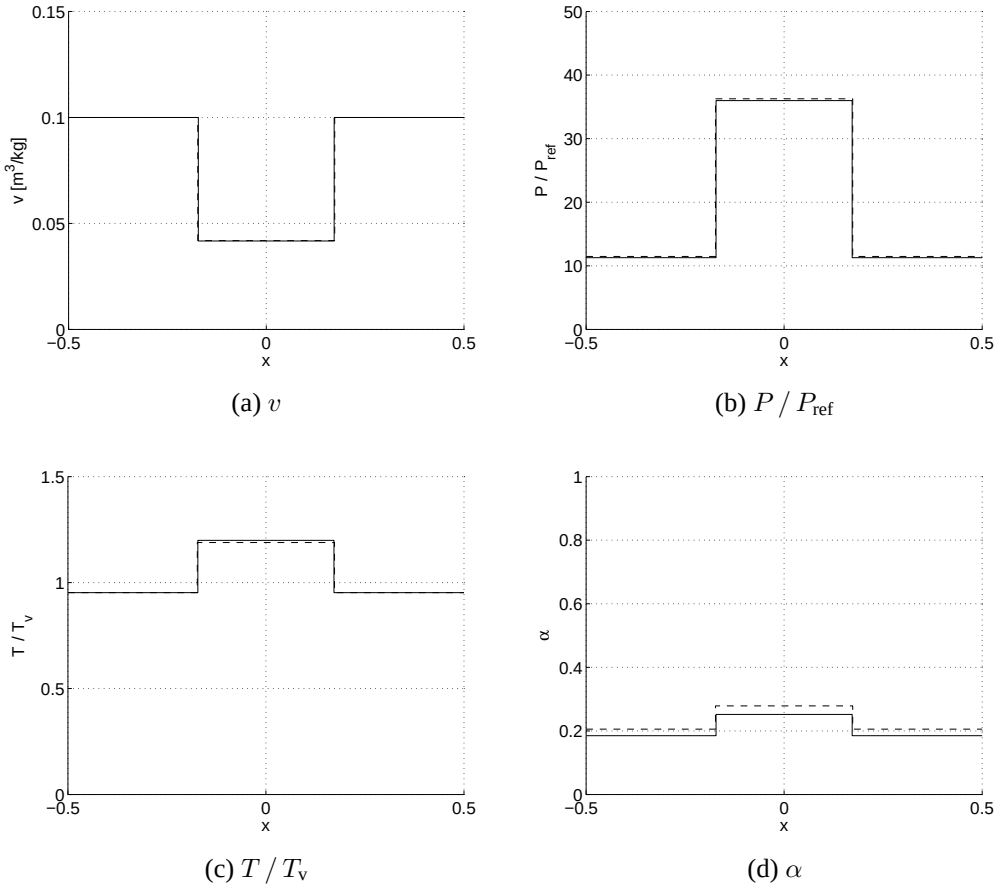

(a) v (b) $P \,/\, P_{\text{ref}}$

(c) $T \,/\, T_{\text{v}}$ (d) α

Figure 12: Two-shock symmetrical solution of the Riemann problem with initial conditions $T_0 = 6000\,\text{K}$, $v_0 = 0.1\,\text{m}^3/\text{kg}$ and $u_0 = \pm 6140\,\text{m/s}$, for the RVD model (solid) and VD model (dashed).

not critical since, for very low temperatures, the parameterized curves representing the thermodynamic properties of the gas overlap and the relative differences on the solutions become independent of v.

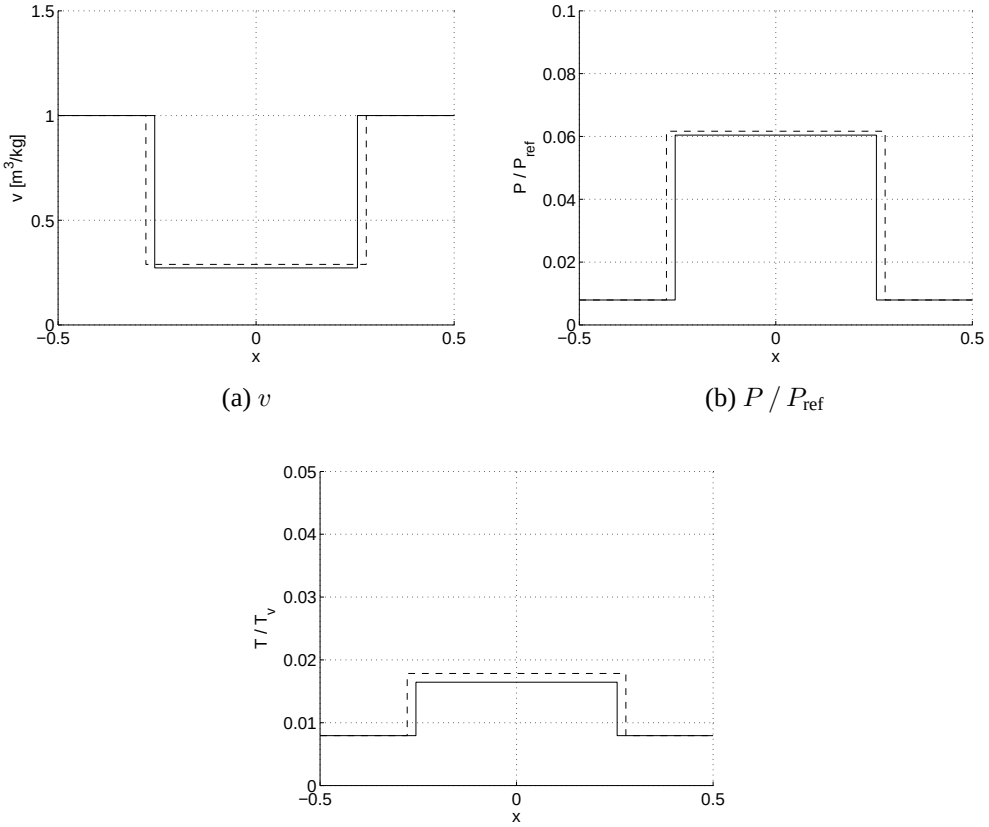

(a) v

(b) $P \,/\, P_{\text{ref}}$

(c) $T \,/\, T_{\text{v}}$

Figure 13: Two-shock symmetrical solution of the Riemann problem with initial conditions $T_0 = 50\,\text{K}$ and $u_0 = \pm 1000\,\text{m/s}$, for the RVD model (solid) and VD model (dashed). The variable α is not shown since for such small temperatures the gas does not dissociate.

5.3 Rarefaction waves

The symmetrical solution with two rarefaction waves needs initial conditions on the two side of the discontinuity characterized by the same thermodynamic states, but opposite diverging velocities. As already pointed out in section 4.4, when two rarefaction waves occur it is possible to have a region of vacuum behind wave's tails. The initial velocities which determine the formation of vacuum depend on the values of the initial thermodynamic properties of the gas, as expressed by equation (4.5).

First, we focus on the domain of initial temperatures in which the rotational motion is fully excited. Values of temperature $1000\,\mathrm{K} < T_0 < 9000\,\mathrm{K}$ and specific volume $0.1\,\mathrm{m}^3/\mathrm{kg} < v < 1000\,\mathrm{m}^3/\mathrm{kg}$ are considered, with initial velocities up to the vacuum formation limit. In all cases the level of dissociation of the gas decreses after the wave. When two rarefaction waves occur, we expect higher differences than with the solution containing two shock waves, due to the integration between the initial condition and the intermediate state which defines the velocities. The analysis of the results confirms that. Differences on all the thermodynamic properties tend to increase with the initial velocity, this means that the more intense is the rarefaction, the higher are the differences between the RVD and VD models. The highest differences are found when the initial gas is partially dissociated. Similarly to the shock waves, they increase with $1/v$. A change in the initial specific volume from $1000\,\mathrm{m}^3/\mathrm{kg}$ to $0.1\,\mathrm{m}^3/\mathrm{kg}$ can triple or more the relative differences on the thermodynamic properties which now reach high values not only for α but also for P, T and v on the contact discontinuity. Figure 14 shows the solution of a Riemann problem in which the rarefaction waves reduce gas dissociation from 40% to 10%. Differences of the values of T, v, P and α in the intermediate state are respectively 2%, 7%, 10% and 14%. For P and α, we notice an increment of the differences with respect to their initial values due to the different thermodynamic models.

Moving the focus on the low temperature region, we notice that the evaluation of the integral (4.3) requires particular attention: 64 Gauss points have been employed to guarantee the requested accuracy. Also, the increment computed by the central Newton iteration have been reduced to avoid negative temperatures. Figure 15 shows the solution of the Riemann problem for $T_0 = 150\,\mathrm{K}$ and $u_0 = \mp 820\,\mathrm{m/s}$. The two models provide very different results, which makes it mandatory to adopt the RVD model in this range of temperatures. The relative difference on the temperature is about 35%. If we observe the specific volume and pressure, differences are much greater. The RVD model provides a value of v in the intermediate state which almost doubles the one provided by the VD model, whereas gives a pressure which is one third of the other.

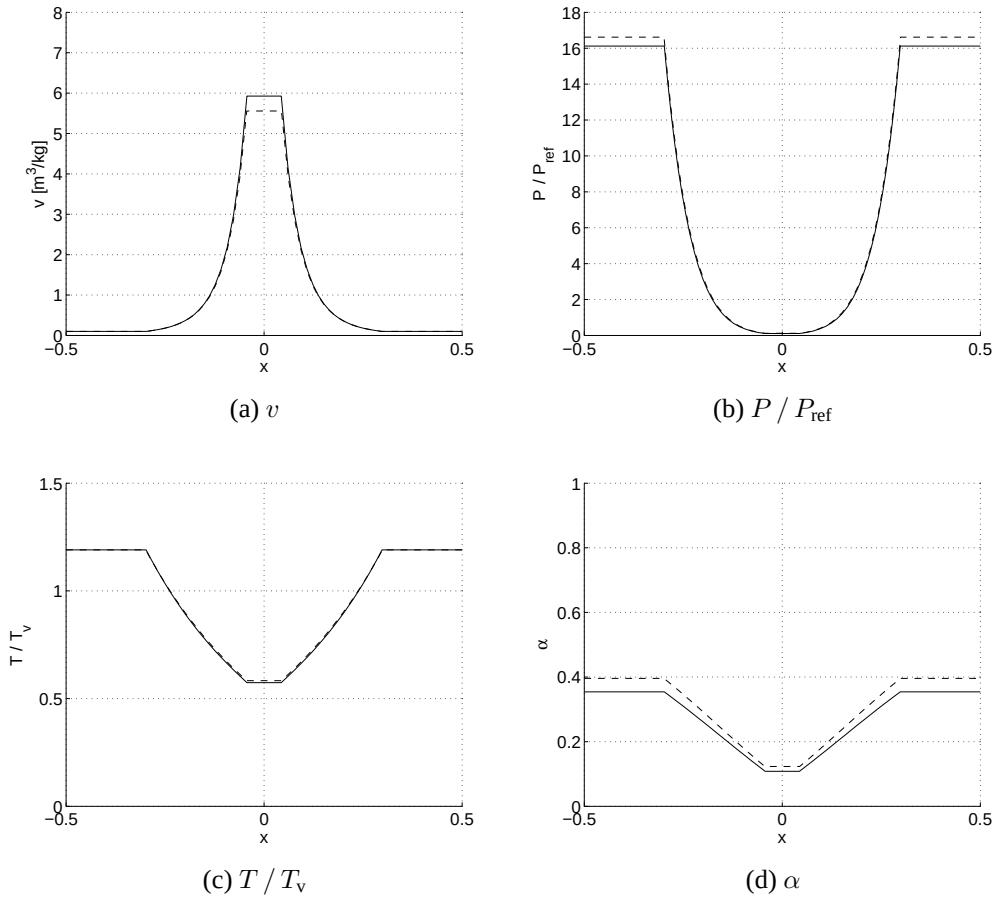

(a) v (b) $P \,/\, P_{\text{ref}}$

(c) $T \,/\, T_{\text{v}}$ (d) α

Figure 14: Two-rarefaction symmetrical solution of the Riemann problem with initial conditions $T_0 = 7500\,\text{K}$, $u_0 = \mp 23000\,\text{m/s}$ and $v = 0.1\,\text{m}^3/\text{kg}$, for the RVD model (solid) and VD model (dashed). The choice of u_0 is such that the gas can encompass the most critical values of α.

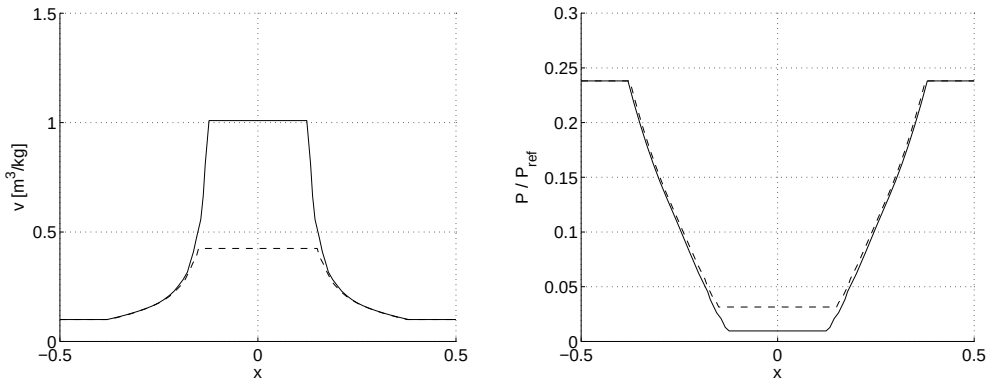

(a) v (b) $P \,/\, P_{\text{ref}}$

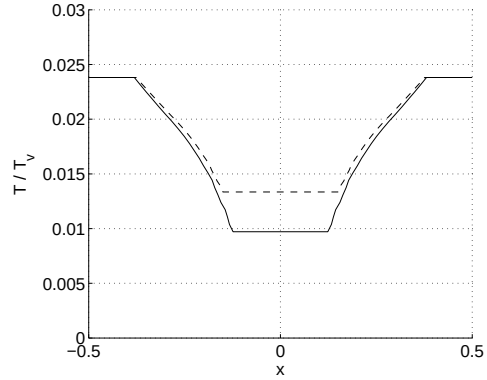

(c) $T \,/\, T_{\text{v}}$

Figure 15: Two-rarefaction symmetrical solution of the Riemann problem with initial conditions $T_0 = 150\,\text{K}$, $u_0 = \mp 820\,\text{m/s}$ and $v = 0.1\,\text{m}^3/\text{kg}$, for the RVD model (solid) and VD model (dashed).

5.4 Mixed solution

Finally, Riemann problems with solutions characterized by the presence of both a shock wave and a rarefaction wave have been solved. This kind of solution is obtained when the initial thermodynamic states are different. The pattern of the waves of the solution is such that the shock wave always propagates towards the region with lower initial temperature or higher initial specific volume.

Initial jumps up to a factor 10 for temperature and 1000 for specific volume have been analyzed. In general, we find that the mixed solution weakens the differences between the solutions provided by the two models which anyhow can be neglected only when the initial jump is very small. The most critical situation is when the initial jump in the specific volume is wery high. Figure 16 shows the Riemann problem solution for $T_0 = 5000\,\mathrm{K}$ and $v_r/v_\ell = 1000$, which produces differences up to 7% on T.

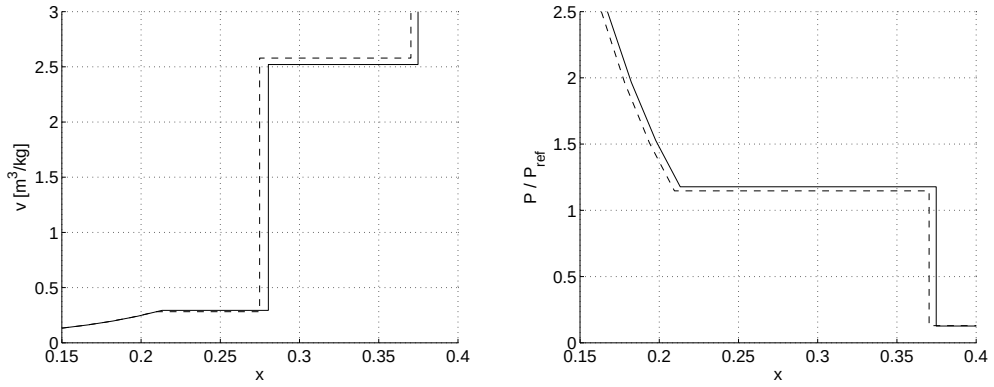

(a) v

(b) $P \,/\, P_{\text{ref}}$

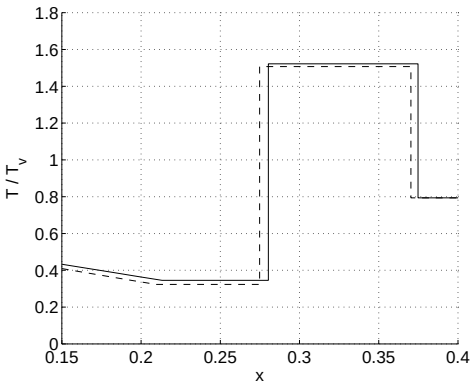

(c) $T \,/\, T_{\text{v}}$

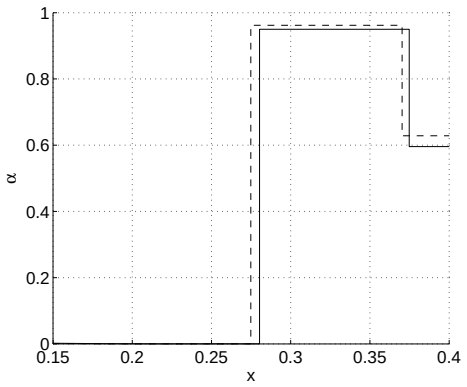

(d) α

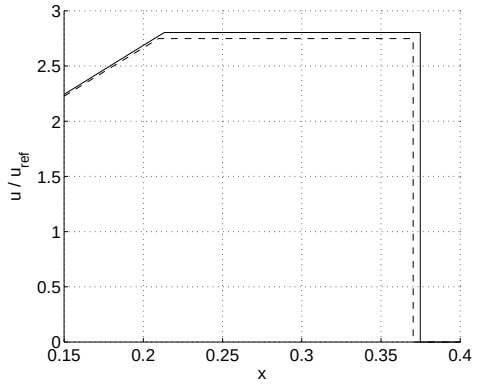

(e) u

Figure 16: Solution of the Riemann problem with initial conditions $T_0 = 5000\,\text{K}$, $v_\ell = 0.01\,\text{m}^3/\text{kg}$ and $v_r = 10\,\text{m}^3/\text{kg}$, for the RVD model (solid) and VD model (dashed).

6 Conclusions

This work conducted a comparison between a completely consistent thermodynamic model (RVD) and two simplified ones (VD and HC) for a mixture consisting of a diatomic molecular gas that can dissociate into atomic constituents. The complete model differs from the others on the treatment of molecular rotations and vibrations, which are completely coupled. The hydrogen gas have been analyzed, because of the high value of its rotational temperature. The thermodynamic properties provided by the complete model have been compared with [9] to verify their accuracy in the low temperature domain in which it gives a completely different description with respect to the simplified models. Also important differences have been found when the gas is only partially dissociated (up to $\alpha \simeq 0.4$), this is emphasized for small values of the specific volume.temperature to

Then, starting from Quartapelle et al. [4], a new formulation of the Riemann problem of gasdynamics for the dissociating gas has been introduced. The presence of the dissociation requires to solve an additional nonlinear problem to have the solution of either the rarefaction wave or the shock wave, which is now computationally more expensive. The Riemann problem has been analyzed for the gas models considered from very small values of the temperature up to complete dissociation and the results obtained by means of the RVD and VD models have been compared. Results for values of temperature for which the rotational motion of the molecule is fully excited, i.e. $T > 300\,\mathrm{K}$, have been considered. Reflecting the initial thermodynamic comparison, the most important differences have been found when the gas is only partially dissociated after the shock or the rarefaction wave. In this case, the choice of the complete model is mandatory to have the correct solution. The analysis of the low temperature region underlines the importance of choosing the complete model which guarantees the correct description of the roto-vibrational molecular motion. For very small temperatures, the RVD and VD models can provide completely different results, especially when two rarefaction waves occur.

Future work should be directed on the confirmation of the numerical results by shock tube experiments as well as on the improvement of the computational efficiency of the solution by a Roe's linearization [16] of the Riemann problem for the dissociating gas to be introduced in the numerical solution schemes by finite volumes. Further work could be aimed at extending the thermodynamic model in order to have a description of an air model valid for hypersonic aerodynamic studies. The application of a H_2 model which allows ionization possibly in the context of relativistic flows represents also a challenge worth of being accepted.

A Partition functions for molecular and atomic hydrogen

In this appendix the partition functions used to derive the properties of both molecular and atomic hydrogen are introduced. In general the partition function is expressed by:

$$\mathcal{Z}(\beta, V, \tilde{N}) = \sum_j \mathrm{e}^{-E_j\beta}, \tag{A.1}$$

where $\beta = 1/(k_{\mathrm{B}}T)$ with $k_{\mathrm{B}} = 1.38065 \times 10^{-23}$ J/K denoting the Boltzmann constant, $\tilde{N}$ the number of the particles contained in the volume V and E_j the total energy of the whole system in the microscopic state j, the summation being extended to all of the possible states of the system. When a system is composed of noninteracting material particles, such as the molecules of an ideal gas, the energy of the system is the sum over the energies of all of its particles. As a consequence, the partition function can be factorized in elementary partition functions of the constituent elements. In particular, for a system of $\tilde{N}$ indistinguishable identical particles, the partition function becomes $\mathcal{Z}(\beta, V, \tilde{N}) = [Z(\beta, V)]^{\tilde{N}}/\tilde{N}!$, where $Z(\beta, V)$ is the partition function of a single molecule.

The energy levels of each single molecule are the eigenvalues of the time independent Schrödinger equation for the whole molecule:

$$\mathcal{H}\psi = E\psi, \tag{A.2}$$

in which ψ is the wavefunction and $\mathcal{H}$ denotes the hamiltonian operator which comprises the total energy of the molecule.

Assuming that the energy of the particle has independent additive contributions, the partition function of the single molecule will assume the factorized form:

$$Z(\beta, V) = \prod_m Z_m(\beta, V) \tag{A.3}$$

In the following, we will give the expression of the partition function of each contribution used express the partition function of the whole molecule H_2 and atom H.

A.1 The hydrogen molecule

A.1.1 Translation

As is well known[3], the translational partition function of a free particle is:

$$Z_{\mathrm{tr}}(T,V) = \left(\frac{2\pi m k_{\mathrm{B}} T}{h^2}\right)^{3/2} V, \tag{A.4}$$

where m denotes the mass of the particle and $h = 6.626068 \times 10^{-34}\,\mathrm{m^2\,kg/s}$ the Planck constant.

A.1.2 Rotation

As a first approximation, the rotations are assumed to be completely independent from the oscillation of the internuclear distance of the molecule. In section A.1.4 the two kinds of motion will be accounted for in a fully coupled model to achieve the correct energy levels.

The rotational energy of the quantum rigid rotor is

$$E_j = j(j+1)k_{\mathrm{B}}T_{\mathrm{r}}, \qquad j = 0, 1, 2\ldots, \tag{A.5}$$

where j is the rotational quantum number and $T_{\mathrm{r}} = \hbar^2/(2\mu r_e^2)$ the *rotational temperature*, with $\hbar = h/(2\pi)$ being the rationalized Planck constant, μ the reduced mass of the molecule and r_e the equilibrium internuclear distance.

For most diatomic molecules, T_{r} assumes a very small value, of the order of few kelvins, while for hydrogen molecule is relatively large $T_{\mathrm{r}} \simeq 88\,\mathrm{K}$. Under the assumption that the rotations are fully excited (the *classical limit*), the rotational partition function becomes:

$$Z_{\mathrm{r}}^{\mathrm{nuc}}(T) = \frac{1}{\sigma_{\mathrm{AB}}}\frac{T}{T_{\mathrm{r}}}, \tag{A.6}$$

with σ_{AB} denoting the symmetry factor, equal to 1 for eteronuclear molecule and 2 for homonuclear, which couples the rotational and nuclear state of atoms. Actually, the expression for the homonuclear case is more complicated and depends on the nuclear spin of the atoms. This will be properly taken into account in section A.1.4.

[3] See any text book dealing with statistical mechanics results or applications such as [8, 10, 17]

A.1.3 Vibration

The simplest way to describe the vibrational motion of a diatomic molecule is using the harmonic oscillator model whose potential is $V(r) = \frac{1}{2}k(r - r_e)^2$, with k denoting the elastic constant and r the distance between atomic nuclei. A closed form solution for the vibrational eigenvalues can be achieved:

$$E_n = \left(n + \frac{1}{2}\right)\hbar\omega_0, \qquad n = 0, 1, 2\ldots, \tag{A.7}$$

with $\omega_0 = \sqrt{k/\mu}$, which are a uniform infinite ladder with separation $\hbar\omega_0$. This model is satisfactory just for small deviations from equilibrium bond length, whereas for larger oscillations the parabolic approximation of the potential must be abandoned. The *Morse potential*, introduced in [3], provides a much more realistic description of molecular potential:

$$V(r) = D_e\left[\left(1 - \mathrm{e}^{-(r-r_e)/\lambda}\right)^2 - 1\right], \qquad \text{for } r > 0, \tag{A.8}$$

where D_e is the potential minimum depth, $r - r_e$ the displacement from the equilibrium distance r_e and λ is a length scale of the Morse potential curve. The three parameters depend on the molecule. The Schrödinger equation with the Morse potential can be solved analytically and leads to the eigenvalues:

$$E_n = -D_e + D_e\left[2 - \left(n + \frac{1}{2}\right)\chi_e\right]\left(n + \frac{1}{2}\right)\chi_e, \quad n = 0, 1, 2\ldots, n_{\text{max}}, \tag{A.9}$$

where $\chi_e = \hbar/(\lambda\sqrt{2\mu D_e}\,)$. Energy levels for the Morse potential are no more distributed with uniform density and tend to be closer as n increases. Notice that the integer values n are limited by a maximum value n_{max} which is obtained from the condition $dE_n/dn = 0$. A direct calculation provides $n_{\text{max}} = 1/\chi_e - 1/2$. It is easy to verify that $E_{n_{\text{max}}} = 0$ and therefore the largest oscillatory Morse mode corresponds to the dissociation of the molecule. Hence, the anharmonic Morse potential provides a valid description of the vibration and dissociation of the diatomic molecule. Figure 17 shows a comparison between the harmonic and the Morse potential.

Finally, the partition function for the Morse oscillator has the following form:

$$Z_{\text{v}}(T) = \sum_{n=0}^{n_{\text{max}}} \mathrm{e}^{-E_n/k_{\text{B}}T} = \mathrm{e}^{D_e/k_{\text{B}}T}\sum_{n=0}^{n_{\text{max}}} \mathrm{e}^{-a_n T_{\text{v}}/T}, \tag{A.10}$$

where we have introduced the shorthand $a_n = \left(n + \frac{1}{2}\right)\left[1 - \left(n + \frac{1}{2}\right)\frac{\chi_e}{2}\right]$ and the *vibrational temperature* $T_{\text{v}} = \hbar\omega_0/k_{\text{B}}$.

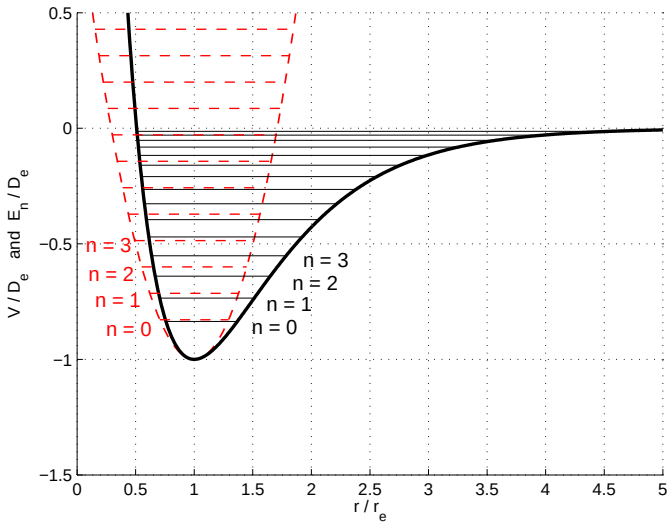

Figure 17: Potential curves and energy levels for the harmonic (red dashed) and Morse (black solid) oscillators.

A.1.4 Roto-vibration

Till now rotational and vibrational degrees of freedom have been considered as completely independent. Overcoming this assumption is mandatory for hydrogen molecule due to the relatively high value of its rotational temperature.

The Schrödinger equation for rotational and vibrational anharmonic motion must be solved. No closed form solution exists, but many approximation techniques[4] can give mathematical expressions of the eigenvalues $E_{n,j}$ which now depend on both rotational and vibrational quantum numbers. The most useful expression of the *roto-vibrational* eigenvalues is the one presented by Harris and Bertolucci [22]:

$$\begin{aligned}\frac{E_{n,j}}{D_e} = &+ \left[1 - j(j+1)(\kappa^2\chi_e)^2\right] j(j+1)(\kappa\chi_e)^2 \\ &- 1 + \left[2 - \left(n+\tfrac{1}{2}\right)\chi_e\right]\left(n+\tfrac{1}{2}\right)\chi_e \\ &- 3j(j+1)\left(n+\tfrac{1}{2}\right)(1-\kappa)(\kappa\chi_e)^3,\end{aligned} \tag{A.11}$$

where $\kappa = \lambda/r_e$, which combines good accuracy and easy usage for our aim.

[4] Some examples can be found in [18, 19, 20, 21].

In order to justify this choice we have compared the values provided by (A.11) with other numerical results (figure 18) as well as with experimental data (figure 19).

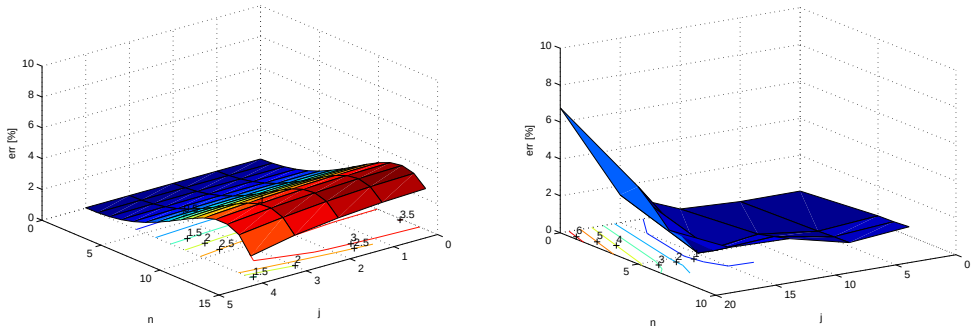

Figure 18: Comparisons between energy levels obtained by means of (A.11) with parameters given by [23] and reproduced in table 1 and numerical results presented in [24] (left plot) and [25] (right plot). Very small relative differences between the models justify the adoption of equation (A.11).

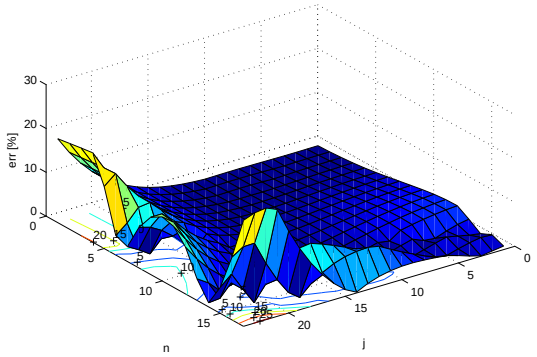

Figure 19: Comparison between energy levels obtained by means of (A.11) and experimental data presented in [26]. Differences are very low for most of the quantum numbers, become relevant just for maximum values of j and n.

In expression (A.11) the levels must be limited by some maximal bound corresponding to the achievement of stationary energy. In the present rotational and vibrational context, to determine the energy stationarity requires to evaluate the partial derivatives $\partial E_{n,j}/\partial n = 0$ and $\partial E_{n,j}/\partial j = 0$ which leads to the cutoff curve presented in figure 20.

Table 1: Morse parameters used for the case of the hydrogen molecule H_2.

state	μ [amu]	λ [Å]	r_e [Å]	$\kappa = \lambda/r_e$	χ_e	D_e [cm^{-1}]
$X^1\sum_g^+$	0.504	0.525	0.741	0.7085	0.0571	38318

Unlike any other diatomic molecule, for which the cutoff is always due to unsustainable vibrations, H_2 dissociates mainly for unsustainable rotations.

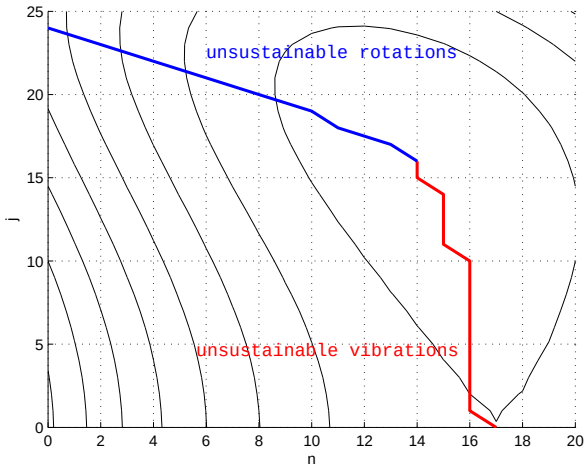

Figure 20: Countour lines of the energy levels and cutoff curve of the roto-vibration spectrum for the hydrogen molecule H_2.

In order to express the roto-vibrational partition function of hydrogen molecule, we have to take into account the coupling between rotation and the nuclear state of atoms in the case of the homonuclear molecule, more complicated than the one expressed in equation (A.6). Following the analysis of Kubo [10], they are coupled through the Fermi statistics since hydrogen nuclei are Fermi particles with half numbered spin. The coupling for the case of the homonuclear molecule is due to symmetry requirement for the nuclear-rotational wave function, in particular it must chance its sign when two Fermi particles are interchanged. The argument leads to the following expression for the nuclear-roto-vibration partition function for the hydrogen molecule:

$$Z_{\mathrm{rv}}^{\mathrm{nuc}}(T) = \mathrm{e}^{D_e/k_{\mathrm{B}}T}(2I_{\mathrm{H}}+1)\sum_{j=0}^{J_{\max}}(I_{\mathrm{H}}+\delta_j)(2j+1)\mathrm{e}^{-\tilde{b}_j/t}\sum_{n=0}^{N_j}\mathrm{e}^{-a_n^j/t} \qquad \text{(A.12)}$$

where $I_{\mathrm{H}} = \frac{1}{2}$ is the hydrogen atom spin number, $t = T/T_{\mathrm{v}}$ is the adimensional tem-

perature, $a_n^j = \left[1 - (n+\frac{1}{2})\frac{\chi_e}{2} - 3j(j+1)(1-\kappa)\kappa\chi_e\frac{T_\mathrm{r}}{T_\mathrm{v}}\right](n+\frac{1}{2})$, $\tilde{b}_j = b_j T_\mathrm{r}/T_\mathrm{v}$ with $b_j = [1 - j(j+1)(\kappa^2\chi_e)^2]\, j(j+1)$ and δ_j a function which is equal to 1 for j odd and 0 for j even.

A.1.5 Electrons

Since the electronic energy levels are largely spaced, the electronic partition function is assumed to contain only the term corresponding to the ground molecular state:

$$Z_\mathrm{el}(T) = g^0 \mathrm{e}^{-E_0/k_\mathrm{B}T}. \tag{A.13}$$

A.1.6 Complete partition function for the molecule

Neglecting the simplest molecule model which consists in consider classical rotations and the harmonic oscillator, we focus on two different models which differ on how rotations are taken into account.

The first model considers the rotational degree of fredom fully excited, hence uses equation (A.6). This avoids the problem of coupling the rotational and internal partition function, as outlined at the end of A.1.2. Thus, the partition function for the whole molecule is:

$$\begin{aligned} Z_{\mathrm{H}_2}(T,V) &= Z^{\mathrm{el}}_{\mathrm{H}_2}(T) Z^{\mathrm{tr}}_{\mathrm{H}_2}(T,V)\, Z^{\mathrm{r,\,nuc}}_{\mathrm{H}_2}(T)\, Z^{\mathrm{v}}_{\mathrm{H}_2}(T) \\ &= g^0_{\mathrm{H}_2} \mathrm{e}^{-E_{0,\mathrm{H}_2}/k_\mathrm{B}T} \left(\frac{2\pi m_{\mathrm{H}_2} k_\mathrm{B} T}{h^2}\right)^{3/2} V \frac{T}{2T^\mathrm{r}_{\mathrm{H}_2}} \mathrm{e}^{D_e/k_\mathrm{B}T} \sum_{n=0}^{n_\mathrm{max}} \mathrm{e}^{-a_n/t}. \end{aligned} \tag{A.14}$$

The second and more physically consistent model considers the complete coupling between rotations and vibrations. The partition function for the whole molecule is:

$$\begin{aligned} Z_{\mathrm{H}_2}(T,V) &= Z^{\mathrm{el}}_{\mathrm{H}_2}(T)\, Z^{\mathrm{tr}}_{\mathrm{H}_2}(T,V)\, Z^{\mathrm{rv,\,nuc}}_{\mathrm{H}_2}(T) \\ &= g^0_{\mathrm{H}_2} \mathrm{e}^{-E_{0,\mathrm{H}_2}/k_\mathrm{B}T} \left(\frac{2\pi m_{\mathrm{H}_2} k_\mathrm{B} T}{h^2}\right)^{3/2} V\, \mathrm{e}^{D_e/k_\mathrm{B}T} (2I_\mathrm{H}+1) \\ &\quad \sum_{j=0}^{J_\mathrm{max}} (I_\mathrm{H} + \delta_j)(2j+1) \mathrm{e}^{-\tilde{b}_j/t} \sum_{n=0}^{N_j} \mathrm{e}^{-a_n^j/t}. \end{aligned} \tag{A.15}$$

A.2 The hydrogen atom

The case of the atomic hydrogen is less complicated than the molecule since there are neihter the rotational nor the vibrational degrees of freedom. The contributions to the partition function come from translational motion and nuclear and electronic coupling. Thus, the partition function for atomic hydrogen is:

$$\begin{aligned} Z_{\mathrm{H}}(T,V) &= Z_{\mathrm{H}}^{\mathrm{tr}}(T,V)\, Z_{\mathrm{H}}^{\mathrm{nuc,\,el}}(T) \\ &= \left(\frac{2\pi m_{\mathrm{H}} k_{\mathrm{B}} T}{h^2}\right)^{3/2} V\ (2I_{\mathrm{H}}+1)\, g_{\mathrm{H}}^{0} \mathrm{e}^{-E_{0,\mathrm{H}}/k_{\mathrm{B}}T}. \end{aligned} \tag{A.16}$$

References

[1] L. Quartapelle and A. Muzzio. *Hydrogen ideal gas thermodynamics with dissociation*. Unpublished, 2010.

[2] L. Quartapelle and F. Auteri. *Fluidodinamica*. Unpublished.

[3] P.M. Morse. Diatomic molecules according to the wave mechanics. II. Vibrational levels. *Physical Review*, 34:57–64, 1929.

[4] L. Quartapelle, L. Castelletti, A. Guardone, and G. Quaranta. Solution of the Riemann problem of classical gasdynamics. *Journal of Computational Physics*, 190:118–140, 2003.

[5] C.G. Miller III and S.E. Wilder. *Table and charts of equilibrium normal-shock properties for pure hydrogen with velocities to* $70\ km/s$, 1976. Langley Research Center, NASA.

[6] H.B. Callen. *Thermodynamics and an Introduction to Thermostatistics*. John Wiley & Sons, Second edition, 1985.

[7] L. Galgani and A. Scotti. On subadditivity and convexity properties of thermodynamic functions. *Pure and Applied Chemistry*, 22:229–235, 1970.

[8] Y.B. Zel'dovich and Y.P. Raizer. *Physics of Shock Waves and High-Temperature Hydrodynamic Phenomena*. Dover Publication, Dover edition, 2002.

[9] R.J. Le Roy, S.G. Chapman, and F.R.W. McCourt. Accurate thermodynamic properties of the six isotopomers of diatomic hydrogen. *Journal of Physical Chemistry*, 94:923–929, 1990.

[10] R. Kubo. *Statistical Mechanics*. North Holland, 1965.

[11] J.W. Leachman, R.T. Jacobsen, S.G. Penoncello, and E.W. Lemmon. Fundamental equations of state for parahydrogen, normal hydrogen, and orthohydrogen. *Journal of Physical and Chemical Reference Data*, 38(9):721–748, 2009.

[12] P.A. Thompson. A fundamental derivative in gasdynamics. *The Physics of Fluids*, 14(9):1843–1849, 1971.

[13] W.G. Vincenti and C.H. Kruger. *Introduction to Physical Gas Dynamics*. Krieger Publishing Company, 1975.

[14] J.D. Anderson Jr. *Hypersonic and High Temperature Gas Dynamics*. AIAA Education, Second edition, 2006.

[15] J.W. Bates and D.C. Montgomery. Some numerical studies of exotic shock wave behaviour. *Physics of Fluids*, 11(2):462–475, 1999.

[16] P.L. Roe. Approximate Riemann solvers, parameter vectors, and difference schemes. *Journal of Computational Physics*, 43(2):357–372, 1981.

[17] P. Atkins and R. Friedman. *Molecular Quantum Mechanics*. Oxford University Press, 2005.

[18] C. Berkdemir and J. Han. Any l-state solutions of the Morse potential through the Pekeris approximation and Nikiforov–Uvarov method. *Chemical Physics Letters*, 409:203–207, 2005.

[19] S.M. Ikhdair. Rotation and vibration of diatomic molecule in the spatially-dependent mass Schrödinger equation with generalized q-deformed Morse potential. *Chemical Physics*, 361:9–17, 2009.

[20] I. Nasser, M.S. Abdelmonem, H. Bahlouli, and A.D. Alhaidari. The rotating Morse potential model for diatomic molecules in the tridiagonal J-matrix representation. *Journal of Physics B*, 40:4245–4257, 2007.

[21] E. Castro, J.L. Paz, and P. Martin. Analytical approximations to the eigenvalues of the Morse potential with centrifugal terms. *Journal of Molecular Structure*, 769:15–18, 2006.

[22] D.C. Harris and M.D. Bertolucci. *Symmetry and Spectroscopy*. Dover Pubblications, 1989.

[23] G.V. Yukhnevich. On application of the Morse potential for Evaluating anharmonic vibrations of polyatomic molecules with XH_n-complexes. *Doklady Physics*, 372(3):322–325, 2000.

[24] D.M. Bishop and S. Shih. An effective Schrödinger equation for the rovibronic energies of H_2 and D_2. *Journal of Chemical Physics*, 64(1):162–169, 1976.

[25] D.A. Morales. Energy eigenstates of the rotating Morse oscillator using the shifted $1/N$ expansion. *Chemical Physics Letters*, 161(3):253–258, 1989.

[26] H.W. Woolley, R.B. Scott, and F.G. Brickwedde. Compilation of the Thermal Properties of Hydrogen in its Various Isotopic and Ortho-Para Modifications. *Journal of Research of the National Bureau of Standards*, 41:379–475, 1948.

[27] R.J. LeVeque. *Numerical Methods for Conservation Laws*. Birkhauser, Second edition, 2008.

[28] L.D. Landau and E.M. Lifshitz. *Fluid Mechanics*. Butterworth-Heinemann, Second edition, 1987.

[29] F.J. Gordillo-Vázquez and J.A. Kunc. Statistical-mechanical calculations of thermal properties of diatomic gases. *Journal of Applied Physics*, 84(9):4693–4703, 1998.

[30] J.P. Killingbeck, A. Grosjean, and G. Jolicard. The Morse potential with angular momentum. *Journal of Chemical Physics*, 116(1):447–448, 2002.